Commun Nonlinear Sci Numer Simulat 132 (2024) 107933

Contents lists available at ScienceDirect

Communications in Nonlinear Science and Numerical Simulation

journal homepage: www.elsevier.com/locate/cnsns

Research paper

Optimal control of a semiclassical Boltzmann equation for charge transport in graphene

Giovanni Nastasi [a,*], Alfio Borzì [b], Vittorio Romano [a]

[a] Dipartimento di Matematica e Informatica, Università degli Studi di Catania, viale Andrea Doria 6, 95125 Catania, Italy
[b] Institut für Mathematik, Universität Würzburg, Emil-Fischer-Strasse 30, 97074 Würzburg, Germany

ARTICLE INFO

MSC:
35Q20
49K20
49M05
65M60

Keywords:
Semiclassical Boltzmann equation
Optimal control theory
Ensemble optimal control problems
Charge transport in graphene
Discontinuous Galerkin scheme

ABSTRACT

An ensemble optimal control problem governed by a semiclassical space-homogeneous Boltzmann equation for charge transport in graphene is formulated and analyzed.

The control mechanism is an external time-dependent electric field having the purpose of driving the material density of electrons in graphene to follow a desired trajectory. For this purpose, an ensemble cost functional with quadratic H^1 costs is considered.

Well-posedness of the control problem is proved, and the characterization of optimal controls by an optimality system is discussed. This system is approximated by a discontinuous Galerkin scheme and solved using a nonlinear conjugate gradient method. Results of numerical experiments are presented that demonstrate the ability of the proposed control framework to design control fields.

1. Introduction

The construction of semiconductor nanostructures requires efficient and accurate methodologies that accommodate physical and engineering details as well as the required functionality of the resulting device. Within this framework, our purpose is to develop a framework for controlling charge transport in graphene for the construction of new devices based on the properties of this material. In fact, some properties of graphene, like high-conductivity and low dimensionality, allow to envision next generation semiconductor technology, which requires to develop control and optimization techniques. We remark that these techniques are key in the design of devices; however, in the field of transport in graphene little effort has been put in the formulation of optimal control strategies.

The purpose of these strategies consists in determining how to optimally change and influence features of the system, which in our case is governed by a semiclassical Boltzmann equation. As in other PDE-constrained optimization problems [1–3], the formulation of corresponding optimal control problems requires to identify a control mechanism and a functional modeling the purpose of the control. These problems are usually solved considering a Lagrange framework that exploits first-order optimality conditions that are formulated in terms of the governing model, its adjoint counterpart, and a gradient equation (or inequality).

The semiclassical Boltzmann equation [4–6] represents an accurate model for graphene simulation that accommodates microscopic effects like electron–electron [6] and electron–phonon [7] interaction. In this model, a natural control mechanism is by an external electric field generated by applied voltage to metallic contacts. With this control, we can manipulate the momentum and current through the graphene in order to perform given tasks. In our work, these tasks are formulated with ensemble cost functionals to be minimized subject to the constraint given by the Boltzmann equation.

* Corresponding author.
E-mail addresses: giovanni.nastasi@unict.it (G. Nastasi), alfio.borzi@mathematik.uni-wuerzburg.de (A. Borzì), romano@dmi.unict.it (V. Romano).

https://doi.org/10.1016/j.cnsns.2024.107933
Received 30 August 2023; Received in revised form 16 January 2024; Accepted 23 February 2024
Available online 24 February 2024

For the simulation of charge transport in graphene, we consider a positivity preserving discontinuous Galerkin (DG) method as discussed in, e.g., [5,8,9]. In [9] the bipolar case has been taken into account; in [4] the electron–electron scattering has been also considered, while in [8] the effects due to the presence of an oxide substrate have been evaluated. In [10], a first attempt to solve the semiclassical Boltzmann equations for charge transport in graphene in a non-homogeneous case has been given. If the carriers are confined in a narrow strip, the so called nanoribbons are obtained and they are simulated in [11]. In [12] thermal effects have been also taken into account.

Regarding optimization in semiconductor materials, an optimal control approach for drift-diffusion equation has been presented in [13,14], and an approach for the MEP energy-transport model has been formulated in [15]. In these works, quadratic cost functionals of tracking type have been investigated. However, in the statistical mechanics framework of the Boltzmann equation, it appears natural to consider ensemble cost functionals [16–20] since they can be interpreted as ensemble averages of potential functions determining the desired mean trajectory and final target. We focus on a space-homogeneous time-dependent electric control field and model its cost in the cost functional with a quadratic H^1 term that guarantees continuous control functions. In the section of numerical experiments, we also present a comparison with the choice of a standard quadratic L^2 regularization term in order to highlight the purpose of our choice.

With the setting defined above, we define the Lagrange function and derive the corresponding optimality system, which results in the governing Boltzmann equation, an adjoint Boltzmann-like model, and an optimality condition equation given by an ordinary differential equation for the control function. Henceforth, we notice that, away from optimality, the residuum of this equation corresponds to the minus gradient of the given constrained optimization problem. Therefore we use this gradient, after appropriate lifting to the H^1 space, to implement a nonlinear conjugate gradient (NCG) technique to solve the optimality system. This choice is motivated by our numerical experience; however, other gradient-based techniques like the so-called BFGS method or a Newton method could be chosen; see, e.g., [1].

We remark that our work is unique in considering an optimal control problem governed by the semiclassical Boltzmann equation for electron transport in graphene. Our contribution is also novel in proposing the class of ensemble cost functionals in the framework of charge transport in graphene. Further, for this setting, we provide the derivation of the optimality system and, in particular, of the adjoint semiclassical Boltzmann equation, which appears in the literature for the first time. Moreover, we present a complete theoretical investigation of the semiclassical Boltzmann equation with a variable external control field. Nonetheless, we remark that this paper represents only the groundwork for developments in a multitude of research directions and therefore it defines a unique benchmark for future work in this field ranging from modeling to numerical issues like the choice of cost functionals and the implementation of other numerical approximation and optimization techniques, respectively.

The plan of the paper is as follows. In Section 2 the semiclassical Boltzmann equation for graphene is introduced. Section 3 is devoted to the theoretical investigation of this partial-integro differential equation. In particular, we prove existence and regularity of solutions in appropriate functional spaces. This section is concluded proving that the control-to-state map is continuous. In Section 4, the ensemble optimal control problem is formulated and a detailed derivation of the optimality system is provided. In Section 5, we illustrate the discontinuous Galerkin approximation of the semiclassical Boltzmann and its adjoint. In Section 6, we discuss the determination of the gradient in the H^1 space, and illustrate the NCG method. In Section 7 results of numerical experiments are reported that validate the effectiveness of the proposed control framework. A section of conclusions completes the exposition of our work. Some details regarding analytical issues are postponed in the appendices.

2. The semiclassical Boltzmann equation

The semiclassical Boltzmann equation for electrons belonging to the conduction band of a graphene layer in the homogeneous case is given by

$$\partial_t f(t,\mathbf{k}) + \mathbf{u}(t)\cdot\nabla_{\mathbf{k}} f(t,\mathbf{k}) = C[f,f](t,\mathbf{k}), \tag{2.1}$$

where $f(t,\mathbf{k})$ is the distribution function of electrons at time $t \geq 0$ and wave-vector $\mathbf{k} \in \mathbb{R}^2$. More precisely, $\mathbf{k}$ belongs to the first Brillouin zone of the crystal lattice [21,22] which is extended to $\mathbb{R}^2$. The time-dependent function $\mathbf{u}(t)$ plays the role of the control variable. From a physical point of view, it is related to an external electric field $\mathbf{E}(t)$ as follows:

$$\mathbf{u}(t) = -\frac{e}{\hbar}\mathbf{E}(t), \tag{2.2}$$

where e is the positive elementary charge and $\hbar$ is the reduced Planck constant. Further, in (2.1), the right-hand side represents the collision term given by

$$C[f,f](t,\mathbf{k}) = \int_{\mathbb{R}^2} S(\mathbf{k}',\mathbf{k}) f(t,\mathbf{k}')(1-f(t,\mathbf{k}))\,d\mathbf{k}' - \int_{\mathbb{R}^2} S(\mathbf{k},\mathbf{k}') f(t,\mathbf{k})(1-f(t,\mathbf{k}'))\,d\mathbf{k}', \tag{2.3}$$

where $S(\mathbf{k}',\mathbf{k})$ is the transition rate for an electron to be scattered from a state of wave-vector $\mathbf{k}'$ to a state of wave-vector $\mathbf{k}$. The presence of the terms $1 - f(t,\mathbf{k})$ and $1 - f(t,\mathbf{k}')$ is due to the Pauli exclusion principle [21].

In the case of graphene, by considering the electron–phonon interaction only, the transition rate reads

$$S(\mathbf{k}',\mathbf{k}) = \sum_{\nu} \left|G^{(\nu)}(\mathbf{k}',\mathbf{k})\right|^2 \left[\left(n_{\mathbf{q}}^{(\nu)}+1\right)\delta\left(\varepsilon(\mathbf{k})-\varepsilon(\mathbf{k}')+\hbar\omega_{\mathbf{q}}^{(\nu)}\right) + n_{\mathbf{q}}^{(\nu)}\delta\left(\varepsilon(\mathbf{k})-\varepsilon(\mathbf{k}')-\hbar\omega_{\mathbf{q}}^{(\nu)}\right)\right], \tag{2.4}$$

where ν indicates the νth phonon mode as described below, $\left|G^{(\nu)}(\mathbf{k}',\mathbf{k})\right|$ is the symmetric matrix element for the scattering mechanism of phonons of type ν. The symbol δ denotes the Dirac distribution and $\varepsilon(\mathbf{k})$ represents the dispersion relation with respect to the Dirac point for electrons in the graphene conduction band [23]:

$$\varepsilon(\mathbf{k}) = \hbar v_F |\mathbf{k}|, \tag{2.5}$$

where v_F is the Fermi velocity. We remark that (2.5) is valid in the proximity of the Dirac points, which is the case we consider. For further details see, e.g., [23]. In (2.4), the quantity $\omega_{\mathbf{q}}^{(\nu)}$ indicates the νth phonon frequency and $n_{\mathbf{q}}^{(\nu)}$ is the Bose–Einstein distribution for the phonon of type ν given by

$$n_{\mathbf{q}}^{(\nu)} = \frac{1}{\exp\left(\hbar\omega_{\mathbf{q}}^{(\nu)}/k_B T\right) - 1}, \tag{2.6}$$

where k_B is the Boltzmann constant and T is the graphene lattice temperature, which in this work is assumed constant.

In graphene the most relevant electron–phonon scatterings are the acoustic (AC), longitudinal optical (LO), transversal optical (TO) and K-phonons. We assume that phonons are at thermal equilibrium. For further information see, e.g., [23–25]. For acoustic phonons, we consider the elastic approximation (see, e.g., [9]) getting

$$2n_{\mathbf{q}}^{(AC)} \left|G^{(AC)}(\mathbf{k}',\mathbf{k})\right|^2 = \frac{1}{(2\pi)^2} \frac{\pi D_{AC} k_B T}{2\hbar\sigma_m v_p^2}(1+\cos\theta_{\mathbf{k},\mathbf{k}'}), \tag{2.7}$$

where D_{AC} is the acoustic phonon coupling constant, v_p is the sound speed in graphene, σ_m the graphene areal density, and $\theta_{\mathbf{k},\mathbf{k}'}$ is the convex angle between $\mathbf{k}$ and $\mathbf{k}'$.

The matrix elements for the optical scatterings write

$$\left|G^{(O)}(\mathbf{k}',\mathbf{k})\right|^2 = \left|G^{(LO)}(\mathbf{k}',\mathbf{k})\right|^2 + \left|G^{(TO)}(\mathbf{k}',\mathbf{k})\right|^2 = \frac{2}{(2\pi)^2} \frac{\pi D_O^2}{\sigma_m \omega_O}, \tag{2.8}$$

and for K-phonons we have

$$\left|G^{(K)}(\mathbf{k}',\mathbf{k})\right|^2 = \frac{1}{(2\pi)^2} \frac{2\pi D_K^2}{\sigma_m \omega_K}(1-\cos\theta_{\mathbf{k},\mathbf{k}'}), \tag{2.9}$$

where D_O is the optical phonon coupling constant, ω_O is the optical phonon frequency, D_K is the K-phonon coupling constant and ω_K is the K-phonon frequency. The summation in (2.4) runs with $\nu = \{AC, LO, TO, K\}$. The numerical values of the physical parameter adopted for the simulations are reported in [26,27].

As initial condition for our Boltzmann model, we assume the equilibrium Fermi–Dirac distribution given by

$$f_0(\mathbf{k}) = \frac{1}{1+\exp\left(\frac{\varepsilon(\mathbf{k})-\varepsilon_F}{k_B T}\right)},$$

where ε_F is the Fermi level evaluated with respect to the Dirac point. From a physical point of view, the Fermi energy is related to the gate potential [28]. In this paper, we choose a Fermi energy large enough to neglect the inter-band scatterings. In [9], it has been shown numerically that a good choice consists to take values larger than 0.2 eV.

Our model can be enriched by many other effects. However, since to the best of our knowledge, this paper is the first attempt to formulate an optimal control problem for a semiclassical Boltzmann equation, we treat the unipolar homogeneous case only.

Notice that the distribution function completely characterizes the statistical properties of the ensemble of electrons in graphene. Therefore all relevant macroscopic quantities can be computed using the distribution as follows:

$$\begin{aligned}
n(t) &= \frac{2}{(2\pi)^2}\int_{\mathbb{R}^2} f(t,\mathbf{k})\,d\mathbf{k},\\
\langle\mathbf{k}\rangle(t) &= \frac{2}{(2\pi)^2}\frac{1}{n(t)}\int_{\mathbb{R}^2} \mathbf{k} f(t,\mathbf{k})\,d\mathbf{k},\\
\langle\mathbf{v}\rangle(t) &= \frac{2}{(2\pi)^2}\frac{1}{n(t)}\int_{\mathbb{R}^2} \mathbf{v}(\mathbf{k}) f(t,\mathbf{k})\,d\mathbf{k},\\
\langle\varepsilon\rangle(t) &= \frac{2}{(2\pi)^2}\frac{1}{n(t)}\int_{\mathbb{R}^2} \varepsilon(\mathbf{k}) f(t,\mathbf{k})\,d\mathbf{k},
\end{aligned}$$

where n is the electron density, $\langle\mathbf{k}\rangle$ is the average crystal momentum, $\langle\mathbf{v}\rangle$ is the mean velocity, $\langle\varepsilon\rangle$ is the mean energy and the factor 2 takes into account the spin degeneracy. The mean velocity is related to the current density by $\mathbf{j}(t) = -e\,n(t)\langle\mathbf{v}\rangle(t)$.

3. Existence and regularity of solutions

In this section and in the Appendix, we theoretically investigate our governing model in the case of regularized transition rates as in [29] and we extend the theoretical results of this work to the case of a controlled semiclassical Boltzmann equation. We consider the following initial-value problem

$$\begin{cases} \partial_t f + \mathbf{u}(t)\cdot\nabla_{\mathbf{k}} f = C_\sigma[f,f] \\ f(0,\mathbf{k}) = f_0(\mathbf{k}) \end{cases} \tag{3.1}$$

where $f = f(t, \mathbf{k}) : [0,T]\times\mathbb{R}^2 \to \mathbb{R}$, $f_0 = f_0(\mathbf{k}) : \mathbb{R}^2 \to \mathbb{R}$ and $\mathbf{u} = \mathbf{u}(t) : [0,T] \to \mathbb{R}^2$, $\mathbf{u} \in H^1(0,T;\mathbb{R}^2)$, with $T > 0$, and the regularized collision term is given by

$$C_\sigma[f,f](t,\mathbf{k}) = \int_{\mathbb{R}^2} S_\sigma(\mathbf{k}',\mathbf{k}) f(t,\mathbf{k}')(1-f(t,\mathbf{k}))\, d\mathbf{k}' - \int_{\mathbb{R}^2} S_\sigma(\mathbf{k},\mathbf{k}') f(t,\mathbf{k})(1-f(t,\mathbf{k}'))\, d\mathbf{k}' , \tag{3.2}$$

where $\sigma > 0$ is a regularization parameter.

We define the following functional space

$$\chi = \left\{ \varphi(\mathbf{k},\mathbf{k}') : \mathbb{R}^2\times\mathbb{R}^2 \to \mathbb{R} \quad \text{s.t.} \quad \varphi \in L^\infty({\mathbb{R}^2}_{\mathbf{k}}, L^1({\mathbb{R}^2}_{\mathbf{k}'})) \quad \text{and} \quad (1+|\mathbf{k}'|^2)^{\gamma/2}\varphi(\mathbf{k},\mathbf{k}') \in L^\infty({\mathbb{R}^2}_{\mathbf{k}'}, L^1({\mathbb{R}^2}_{\mathbf{k}})) \right\}, \tag{3.3}$$

with $\gamma > 2$.

We assume that the regularized transition rates $S_\sigma(\mathbf{k},\mathbf{k}')$ and the initial distribution f_0 satisfy the following conditions

(A1) $S_\sigma(\mathbf{k},\mathbf{k}') \geq 0, \quad S_\sigma(\mathbf{k},\mathbf{k}') \in \chi,$
(A2) $|\nabla_{\mathbf{k}} S_\sigma(\mathbf{k},\mathbf{k}')| \in \chi, \quad |\nabla_{\mathbf{k}'} S_\sigma(\mathbf{k},\mathbf{k}')| \in \chi,$
(A3) $0 \leq f_0 \leq 1, \quad f_0 \in W^{1,1}(\mathbb{R}^2), \quad (1+|\mathbf{k}|^2)^{\gamma/2}(|f_0| + |\nabla_{\mathbf{k}} f_0|) \in L^\infty(\mathbb{R}^2).$

With this preparation, we can state the following result, which is proved in Appendix A.

Theorem 1. *We assume that the conditions (A1)-(A3) hold. Then the problem (3.1) admits a unique solution such that*

(i) $0 \leq f(t,\mathbf{k}) \leq 1, \quad (t,\mathbf{k}) \in [0,T]\times\mathbb{R}^2,$
(ii) $f \in L^\infty\left((0,T), W^{1,1}(\mathbb{R}^2)\right),$
(iii) $(1+|\mathbf{k}|^2)^{\gamma/2}(|f| + |\nabla_{\mathbf{k}} f|) \in L^\infty((0,T), L^\infty(\mathbb{R}^2)).$

With this result and the initial condition fixed, we can state the well-posedness of the control-to-state map $\mathbf{u} \mapsto f = \mathcal{G}(\mathbf{u})$, where

$$\mathcal{G} : H^1(0,T;\mathbb{R}^2) \to L^\infty\left((0,T), W^{1,1}(\mathbb{R}^2)\right).$$

Therefore $f = \mathcal{G}(\mathbf{u})$ represents the unique solution to (3.1) for a given $\mathbf{u}$. The continuity of this map is assured by what follows.

Proposition 1. *Assume that the conditions (A1)-(A3) hold. Then the control-to-state map $\mathbf{u} \mapsto f = \mathcal{G}(\mathbf{u})$ for (3.1) is Lipschitz continuous as follows:*

$$\left\| f_1(t,\mathbf{k}) - f_2(t,\mathbf{k}) \right\|_{L^1(\mathbb{R}^2)} \leq C \left\| \mathbf{u}_1 - \mathbf{u}_2 \right\|_\infty , \tag{3.4}$$

where $\mathbf{u}_1$, $\mathbf{u}_2 \in H^1(0,T;\mathbb{R}^2)$ and f_1, f_2 are the corresponding solutions; $C = C(S_\sigma, T)$.

For the proof, see Appendix B.

Remark 1. We remark that, in our theoretical analysis, a regularized transition rate S_σ is considered, which can be obtained from (2.4) by replacing the Dirac delta function [30] with a positive symmetric mollifier (e.g., using the normalized bump function). On the other hand, notice that the transition rate (2.4) is obtained in a limiting process based on the Dirac–Fermi's golden rule [21]. Therefore, in our context, the natural approximation to the Dirac delta is the following function

$$\delta_\sigma(x) = \frac{\sin^2(x/\sigma)}{\pi x^2/\sigma}\rho,$$

such that $\delta_\sigma(x) \approx \delta(x)$ as σ approaches zero, where $\rho(x)$ is a smoothed characteristic function that guarantees boundness and integrability of the regularized transition rate S_σ.

4. Formulation of the optimal control problem

We consider the problem of determining a control field that drives the ensemble of electrons in graphene in order to perform a given task in an optimal way. In mathematical terms, this modeling step consists in the definition of an objective functional to be minimized (or maximized) subject to the differential constraint given by our Boltzmann model.

Specifically, we formulate the task of steering the ensemble of particles to follow a given trajectory and reach a desired final configuration. In our statistical framework, this objective can be achieved requiring to minimize the expected value of valley potentials supported on the desired trajectory and final state. On the other hand, for optimal performance we also require to minimize the cost of the control. These two objectives can be encoded in the following functional

$$J(f,\mathbf{u}) = \int_0^T \int_{\mathbb{R}^2} \theta(t,\mathbf{k}) f(t,\mathbf{k})\, d\mathbf{k}\, dt + \int_{\mathbb{R}^2} \varphi(\mathbf{k}) f(T,\mathbf{k})\, d\mathbf{k} + \frac{\nu}{2} \|\mathbf{u}\|^2_{H^1_T} , \tag{4.1}$$

where

$$\|\mathbf{u}\|^2_{H^1_T} = \int_0^T |\mathbf{u}(t)|^2\, dt + \int_0^T \left| \frac{d}{dt}\mathbf{u}(t) \right|^2 dt.$$

Notice that the weight of the cost of the control $\nu > 0$ allows to set a trade-off between the two objectives.

In (4.1), in the first term (tracking) the function θ represents an attracting potential for the electrons to have wave-vectors as close as possible to the minimum of θ for any fixed t. Thus, we may choose $\theta(t,\mathbf{k}) = \Theta(|\mathbf{k}-\mathbf{k}_d(t)|)$ such that the global minimum of the tracking part is achieved when all particles have at time t the wave-vector $\mathbf{k}_d(t)$. In our experiments, we choose

$$\theta(t,\mathbf{k}) = -\frac{1}{1+\exp\left(\frac{\hbar v_F|\mathbf{k}-\mathbf{k}_d(t)|-\varepsilon_F}{k_B T}\right)},$$

and $\varphi(\mathbf{k}) = \theta(T,\mathbf{k})$.

Similarly, the final observation term can be defined as $\varphi(\mathbf{k}) = \Phi(|\mathbf{k}-\mathbf{k}_T|)$, which may correspond to the requirement that, in average, the wave-vectors of the particles at final time are close to $\mathbf{k}_T$. In general, we require that θ and φ are bounded from below, radially monotonically growing, integrable, and locally convex in the neighborhood of $\mathbf{k}_d$ and $\mathbf{k}_T$, respectively.

The third term in (4.1) represents the cost of the control, which in this case is the square of the $H^1(0,T)$ norm of $\mathbf{u}$. This cost was proposed in [31] based on the concept of minimum attention control in the sense that slow varying controls are promoted in the minimization process. In fact, because of the continuous embedding $H^1(0,T) \hookrightarrow C([0,T])$, the optimal control obtained with our formulation is continuous.

With this preparation, we formulate our ensemble optimal control problem as follows:

$$\min J(f,\mathbf{u}) := \int_0^T \int_{\mathbb{R}^2} \theta(t,\mathbf{k}) f(t,\mathbf{k})\, d\mathbf{k}\, dt + \int_{\mathbb{R}^2} \varphi(\mathbf{k}) f(T,\mathbf{k})\, d\mathbf{k} + \frac{\nu}{2}\, \|\mathbf{u}\|^2_{H^1_T} \tag{4.2a}$$

$$s.t. \qquad \partial_t f(t,\mathbf{k}) + \mathbf{u}(t)\cdot\nabla_{\mathbf{k}} f(t,\mathbf{k}) = C[f,f](t,\mathbf{k}), \qquad f(0,\mathbf{k}) = f_0(\mathbf{k}), \tag{4.2b}$$

where $\mathbf{u} \in H^1(0,T;\mathbb{R}^2)$, and 's.t.' means subject to.

Next, we remark that with the control-to-state map $\mathcal{G}$, we can define the reduced cost functional $J_r(\mathbf{u}) := J(\mathcal{G}(\mathbf{u}),\mathbf{u})$ and consider the equivalent formulation of (4.2) as follows

$$\min_{\mathbf{u}\in H^1(0,T;\mathbb{R}^2)} J_r(\mathbf{u}),$$

which has the structure of an unconstrained optimization problem.

Now, as in [16], based on the properties of θ and φ, the statements of Theorem 1 on the density f, the coercivity of J with respect to $\mathbf{u}$ in $H^1(0,T;\mathbb{R}^2)$, and the Lipschitz continuity of the control to state map, we can state existence of solutions to our optimal control problem.

Once the existence of optimal controls is established, we can focus on their characterization by means of first-order optimality conditions. Assuming Fréchet differentiability of J and $\mathcal{G}$, if $\mathbf{u}$ is optimal, then it must satisfy $\nabla_{\mathbf{u}} J_r(\mathbf{u}) = 0$, where $\nabla_{\mathbf{u}}$ denotes the gradient in the Hilbert space $H^1(0,T;\mathbb{R}^2)$.

Based on the Lagrange framework, the optimality condition $\nabla_{\mathbf{u}} J_r(\mathbf{u}) = \mathbf{0}$ can be conveniently rewritten in terms of an optimality system consisting of our governing Boltzmann model, the corresponding optimization adjoint, and an optimality equation for the control. This system can be obtained in terms of extremal conditions of the following Lagrange functional

$$\mathcal{L}(f,\mathbf{u},q) = J(f,\mathbf{u}) + \int_0^T \int_{\mathbb{R}^2} \left(\partial_t f + \mathbf{u}\cdot\nabla_{\mathbf{k}} f - C[f,f]\right) q\, d\mathbf{k}\, dt\,,$$

where $q(t,\mathbf{k})$ represents the Lagrange multiplier. Notice that the second term in this functional corresponds to the L^2 scalar product in $Q = [0,T]\times\mathbb{R}^2$; we denoted this product with $(\cdot,\cdot)$. In this space, we determine the gradients of $\mathcal{L}$ with respect to q, $\mathbf{u}$ and f and require that they are zero at the extremals of the Lagrange functional. These gradients can be conveniently computed considering Gâteaux derivatives as follows.

For the Gâteaux derivative of $\mathcal{L}$ with respect to q we have

$$\begin{aligned}(\nabla_q \mathcal{L}, \delta q) &= \lim_{h\to 0^+} \frac{1}{h}\left[\mathcal{L}(f,\mathbf{u},q+h\delta q) - \mathcal{L}(f,\mathbf{u},q)\right]\\ &= \lim_{h\to 0^+} \frac{1}{h}\left[\int_0^T \int_{\mathbb{R}^2} \left(\partial_t f + \mathbf{u}\cdot\nabla_{\mathbf{k}} f - C[f,f]\right)(q+h\delta q)\, d\mathbf{k}\, dt \right.\\ &\left. - \int_0^T \int_{\mathbb{R}^2} \left(\partial_t f + \mathbf{u}\cdot\nabla_{\mathbf{k}} f - C[f,f]\right) q\, d\mathbf{k}\, dt\right]\\ &= \int_0^T \int_{\mathbb{R}^2} \left(\partial_t f + \mathbf{u}\cdot\nabla_{\mathbf{k}} f - C[f,f]\right) \delta q\, d\mathbf{k}\, dt.\end{aligned}$$

Therefore $\nabla_q \mathcal{L} := \partial_t f + \mathbf{u}\cdot\nabla_{\mathbf{k}} f - C[f,f]$. By requiring $(\nabla_q \mathcal{L}, \delta q) = 0$ for all variations δq, we obtain our governing model.

Next, we compute the Gateaux derivative with respect to $\mathbf{u}$. We have

$$\begin{aligned}(\nabla_{\mathbf{u}} \mathcal{L}, \delta\mathbf{u}) &= \lim_{h\to 0^+} \frac{1}{h}\left[\mathcal{L}(f,\mathbf{u}+h\delta\mathbf{u},q) - \mathcal{L}(f,\mathbf{u},q)\right]\\ &= \nu \int_0^T \mathbf{u}\cdot\delta\mathbf{u}\, dt + \nu \int_0^T \mathbf{u}'(t)\cdot\delta\mathbf{u}'(t)\, dt + \int_0^T \int_{\mathbb{R}^2} (\delta\mathbf{u}\cdot\nabla_{\mathbf{k}} f) q\, d\mathbf{k}\, dt\\ &= \nu \int_0^T \mathbf{u}\cdot\delta\mathbf{u}\, dt + \nu \left[\mathbf{u}'\cdot\delta\mathbf{u}\right]_0^T - \nu \int_0^T \mathbf{u}''\cdot\delta\mathbf{u}\, dt + \int_0^T \int_{\mathbb{R}^2} (\delta\mathbf{u}\cdot\nabla_{\mathbf{k}} f) q\, d\mathbf{k}\, dt\end{aligned}$$

$$= \int_0^T \left(\nu\mathbf{u} - \nu\,\mathbf{u}'' + \int_{\mathbb{R}^2} q\nabla_{\mathbf{k}} f \, d\mathbf{k} \right) \cdot \delta\mathbf{u}\, dt,$$

where $\mathbf{u}' := \frac{d}{dt}\mathbf{u}(t)$ and $\mathbf{u}'' := \frac{d^2}{dt^2}\mathbf{u}(t)$.

Notice that, in this derivation, we make the modeling assumption that $\mathbf{u}(0) = \mathbf{0}$ and $\mathbf{u}(T) = \mathbf{0}$. This is a modeling choice corresponding to the assumption that the control is switched on at $t = 0$ and off at $t = T$. This setting would not be possible in the case of a L^2 regularization term. Notice that the resulting equation

$$\nu\,\mathbf{u}(t) - \nu\,\mathbf{u}''(t) + \int_{\mathbb{R}^2} q(t,\mathbf{k})\,\nabla_{\mathbf{k}} f(t,\mathbf{k})\, d\mathbf{k} = \mathbf{0},$$

should be understood in weak sense. We remark that the left-hand side of this equation corresponds to the $L^2(0,T;\mathbb{R}^2)$ gradient of the reduced cost functional, that is,

$$\nabla_{\mathbf{u}} J_r(\mathbf{u}) = \nu\,\mathbf{u} - \nu\,\mathbf{u}'' + \int_{\mathbb{R}^2} q\,\nabla_{\mathbf{k}} f\, d\mathbf{k}. \tag{4.3}$$

Next, we derive the adjoint Boltzmann equation that corresponds to the requirement $(\nabla_f \mathcal{L}, \delta f) = 0$ for all admissible variations δf. Since this model is new in the scientific literature, we present all details of its derivation. We have

$$\begin{aligned}
(\nabla_f \mathcal{L}, \delta f) &= \lim_{h\to 0^+} \frac{1}{h}\left[\mathcal{L}(f+\delta f, \mathbf{u}, q) - \mathcal{L}(f,\mathbf{u},q)\right] \\
&= \lim_{h\to 0^+} \frac{1}{h}\Bigg[\int_0^T \int_{\mathbb{R}^2} \theta(t,\mathbf{k})(f(t,\mathbf{k}) + h\delta f(t,\mathbf{k}))\, d\mathbf{k}\, dt - \int_0^T \int_{\mathbb{R}^2} \theta(t,\mathbf{k}) f(t,\mathbf{k})\, d\mathbf{k}\, dt \\
&+ \int_0^T \int_{\mathbb{R}^2} \big(\partial_t (f + h\delta f) + \mathbf{u}\cdot\nabla_{\mathbf{k}}(f + h\delta f) - C[f + h\delta f, f + h\delta f]\big)\, q\, d\mathbf{k}\, dt \\
&- \int_0^T \int_{\mathbb{R}^2} \big(\partial_t f + \mathbf{u}\cdot\nabla_{\mathbf{k}} f - C[f,f]\big)\, q\, d\mathbf{k}\, dt \\
&+ \int_{\mathbb{R}^2} \varphi(\mathbf{k})\,(f(T,\mathbf{k}) + h\delta f(T,\mathbf{k}))\, d\mathbf{k} - \int_{\mathbb{R}^2} \varphi(\mathbf{k})\, f(T,\mathbf{k})\, d\mathbf{k}\Bigg].
\end{aligned}$$

Moreover, since

$$\begin{aligned}
&\int_0^T \int_{\mathbb{R}^2} \partial_t \delta f\, q\, d\mathbf{k}\, dt = \int_{\mathbb{R}^2} [q\delta f]_0^T\, d\mathbf{k} - \int_0^T \int_{\mathbb{R}^2} \partial_t q\, \delta f\, d\mathbf{k}\, dt \\
&= \int_{\mathbb{R}^2} q(T,\mathbf{k})\,\delta f(T,\mathbf{k})\, d\mathbf{k} - \int_{\mathbb{R}^2} q(0,\mathbf{k})\delta f(0,\mathbf{k})\, d\mathbf{k} - \int_0^T \int_{\mathbb{R}^2} \partial_t q\,\delta f\, d\mathbf{k}\, dt \\
&= \int_{\mathbb{R}^2} q(T,\mathbf{k})\,\delta f(T,\mathbf{k})\, d\mathbf{k} - \int_0^T \int_{\mathbb{R}^2} \partial_t q\,\delta f\, d\mathbf{k}\, dt,
\end{aligned}$$

where the last step is obtained because of the fixed initial condition so that $\delta f(0,\mathbf{k}) = 0$ for all $\mathbf{k}\in\mathbb{R}^2$, and

$$\int_0^T \int_{\mathbb{R}^2} (\mathbf{u}\cdot\nabla_{\mathbf{k}}\delta f)\, q\, d\mathbf{k}\, dt = -\int_0^T \int_{\mathbb{R}^2} (\mathbf{u}\cdot\nabla_{\mathbf{k}} q)\,\delta f\, d\mathbf{k}\, dt,$$

because of the decay of δf to zero for $|\mathbf{k}| \to +\infty$, we have

$$\begin{aligned}
(\nabla_f \mathcal{L}, \delta f) &= \int_0^T \int_{\mathbb{R}^2} \theta(t,\mathbf{k})\,\delta f(t,\mathbf{k})\, d\mathbf{k}\, dt \\
&+ \int_{\mathbb{R}^2} (q(T,\mathbf{k}) + \varphi(\mathbf{k}))\,\delta f(T,\mathbf{k})\, d\mathbf{k} - \int_0^T \int_{\mathbb{R}^2} \partial_t q\,\delta f\, d\mathbf{k}\, dt - \int_0^T \int_{\mathbb{R}^2} (\mathbf{u}\cdot\nabla_{\mathbf{k}} q)\delta f\, d\mathbf{k}\, dt \\
&- \lim_{h\to 0^+} \frac{1}{h}\left[\int_0^T \int_{\mathbb{R}^2} (C[f + h\delta f, f + h\delta f] - C[f,f])\, q\, d\mathbf{k}\, dt\right].
\end{aligned}$$

Now, we focus on the collision term

$$\begin{aligned}
&C[f + h\delta f, f + h\delta f] - C[f,f] \\
&= \int_{\mathbb{R}^2} S(\mathbf{k}',\mathbf{k})(f + h\delta f)(t,\mathbf{k}')(1 - (f + h\delta f)(t,\mathbf{k}))\, d\mathbf{k}' \\
&- \int_{\mathbb{R}^2} S(\mathbf{k},\mathbf{k}')(f + h\delta f)(t,\mathbf{k})(1 - (f + h\delta f)(t,\mathbf{k}'))\, d\mathbf{k}' \\
&- \int_{\mathbb{R}^2} S(\mathbf{k}',\mathbf{k}) f(t,\mathbf{k}')(1 - f(t,\mathbf{k}))\, d\mathbf{k}' + \int_{\mathbb{R}^2} S(\mathbf{k},\mathbf{k}') f(t,\mathbf{k})(1 - f(t,\mathbf{k}'))\, d\mathbf{k}' \\
&= \int_{\mathbb{R}^2} S(\mathbf{k}',\mathbf{k})(f(\mathbf{k}')(1 - f(\mathbf{k})) - hf(\mathbf{k}')\delta f(\mathbf{k}) + h\delta f(\mathbf{k}')(1 - f(\mathbf{k})) - h^2\delta f(\mathbf{k}')\delta f(\mathbf{k}))\, d\mathbf{k}' \\
&- \int_{\mathbb{R}^2} S(\mathbf{k},\mathbf{k}')(f(\mathbf{k})(1 - f(\mathbf{k}')) - hf(\mathbf{k})\delta f(\mathbf{k}') + h\delta f(\mathbf{k})(1 - f(\mathbf{k}')) - h^2\delta f(\mathbf{k})\delta f(\mathbf{k}'))\, d\mathbf{k}'
\end{aligned}$$

$$
\begin{aligned}
&- \int_{\mathbb{R}^2} S(\mathbf{k}',\mathbf{k}) f(t,\mathbf{k}')(1-f(t,\mathbf{k}))\,d\mathbf{k}' + \int_{\mathbb{R}^2} S(\mathbf{k},\mathbf{k}') f(t,\mathbf{k})(1-f(t,\mathbf{k}'))\,d\mathbf{k}' \\
&= \int_{\mathbb{R}^2} S(\mathbf{k}',\mathbf{k})(-hf(\mathbf{k}')\delta f(\mathbf{k}) + h\delta f(\mathbf{k}')(1-f(\mathbf{k})) - h^2 \delta f(\mathbf{k}')\delta f(\mathbf{k}))\,d\mathbf{k}' \\
&- \int_{\mathbb{R}^2} S(\mathbf{k},\mathbf{k}')(-hf(\mathbf{k})\delta f(\mathbf{k}') + h\delta f(\mathbf{k})(1-f(\mathbf{k}')) - h^2 \delta f(\mathbf{k})\delta f(\mathbf{k}'))\,d\mathbf{k}'.
\end{aligned}
$$

Therefore we get

$$
\begin{aligned}
&\int_0^T \int_{\mathbb{R}^2} \lim_{h\to 0^+} \frac{1}{h} \left[C[f+h\delta f, f+h\delta f] - C[f,f]\right] q\,d\mathbf{k}\,dt \\
&= \int_0^T \int_{\mathbb{R}^2} \left[\int_{\mathbb{R}^2} S(\mathbf{k}',\mathbf{k})(-f(\mathbf{k}')\delta f(\mathbf{k}) + \delta f(\mathbf{k}')(1-f(\mathbf{k})))\,d\mathbf{k}' \right.\\
&\left. - \int_{\mathbb{R}^2} S(\mathbf{k},\mathbf{k}')(-f(\mathbf{k})\delta f(\mathbf{k}') + \delta f(\mathbf{k})(1-f(\mathbf{k}')))\,d\mathbf{k}'\right] q\,d\mathbf{k}\,dt \\
&= \int_0^T \left\{ \int_{\mathbb{R}^2} \left[\int_{\mathbb{R}^2} -S(\mathbf{k}',\mathbf{k}) f(\mathbf{k}')\delta f(\mathbf{k}) - S(\mathbf{k},\mathbf{k}')\delta f(\mathbf{k})(1-f(\mathbf{k}'))\,d\mathbf{k}'\right] q(\mathbf{k})\,d\mathbf{k} \right.\\
&\left. + \int_{\mathbb{R}^2} \left[\int_{\mathbb{R}^2} S(\mathbf{k}',\mathbf{k})\delta f(\mathbf{k}')(1-f(\mathbf{k})) - S(\mathbf{k},\mathbf{k}')(-f(\mathbf{k}))\delta f(\mathbf{k}')\,d\mathbf{k}'\right] q(\mathbf{k})\,d\mathbf{k} \right\} dt \\
&= \int_0^T \left\{ \int_{\mathbb{R}^2}\int_{\mathbb{R}^2} \left[-S(\mathbf{k}',\mathbf{k}) f(\mathbf{k}')\delta f(\mathbf{k}) - S(\mathbf{k},\mathbf{k}')\delta f(\mathbf{k})(1-f(\mathbf{k}'))\right] q(\mathbf{k})\,d\mathbf{k}'\,d\mathbf{k} \right.\\
&\left. + \int_{\mathbb{R}^2}\int_{\mathbb{R}^2} \left[S(\mathbf{k},\mathbf{k}')\delta f(\mathbf{k})(1-f(\mathbf{k}')) - S(\mathbf{k}',\mathbf{k})(-f(\mathbf{k}'))\delta f(\mathbf{k})\right] q(\mathbf{k}')\,d\mathbf{k}'\,d\mathbf{k} \right\} dt \\
&= \int_0^T \int_{\mathbb{R}^2} \delta f(\mathbf{k}) \int_{\mathbb{R}^2} [S(\mathbf{k}',\mathbf{k})(-f(\mathbf{k}')q(\mathbf{k}) + f(\mathbf{k}')q(\mathbf{k}')) \\
&+ S(\mathbf{k},\mathbf{k}')(-(1-f(\mathbf{k}'))q(\mathbf{k}) + (1-f(\mathbf{k}'))q(\mathbf{k}'))]\,d\mathbf{k}'\,d\mathbf{k}\,dt \\
&= \int_0^T \int_{\mathbb{R}^2} \delta f(\mathbf{k}) \left[\int_{\mathbb{R}^2} S(\mathbf{k}',\mathbf{k}) f(\mathbf{k}')(q(\mathbf{k}') - q(\mathbf{k}))\,d\mathbf{k}' \right.\\
&\left. + \int_{\mathbb{R}^2} S(\mathbf{k},\mathbf{k}')(1-f(\mathbf{k}'))(q(\mathbf{k}') - q(\mathbf{k}))\,d\mathbf{k}'\right] d\mathbf{k}\,dt.
\end{aligned}
$$

Finally, we obtain

$$
\begin{aligned}
(\nabla_f \mathcal{L}, \delta f) &= \int_0^T \int_{\mathbb{R}^2} \theta(t,\mathbf{k})\delta f\,d\mathbf{k}\,dt \\
&+ \int_{\mathbb{R}^2} (q(T,\mathbf{k}) + \varphi(\mathbf{k}))\,\delta f(T,\mathbf{k})\,d\mathbf{k} - \int_0^T \int_{\mathbb{R}^2} \partial_t q\,\delta f\,d\mathbf{k}\,dt - \int_0^T \int_{\mathbb{R}^2} (\mathbf{u}\cdot\nabla_{\mathbf{k}} q)\delta f\,d\mathbf{k}\,dt \\
&- \int_0^T \int_{\mathbb{R}^2} \delta f(t,\mathbf{k}) \left[\int_{\mathbb{R}^2} S(\mathbf{k},\mathbf{k}') f(\mathbf{k}')(q(t,\mathbf{k}') - q(t,\mathbf{k}))\,d\mathbf{k}' \right.\\
&\left. + \int_{\mathbb{R}^2} S(\mathbf{k}',\mathbf{k})(1-f(\mathbf{k}'))(q(t,\mathbf{k}') - q(t,\mathbf{k}))\,d\mathbf{k}'\right] d\mathbf{k} \\
&= \int_0^T \int_{\mathbb{R}^2} \left[\theta(t,\mathbf{k}) - \partial_t q - \mathbf{u}\cdot\nabla_{\mathbf{k}} q - \int_{\mathbb{R}^2} S(\mathbf{k}',\mathbf{k}) f(\mathbf{k}')(q(t,\mathbf{k}') - q(t,\mathbf{k}))\,d\mathbf{k}' \right.\\
&\left. - \int_{\mathbb{R}^2} S(\mathbf{k},\mathbf{k}')(1-f(\mathbf{k}'))(q(t,\mathbf{k}') - q(t,\mathbf{k}))\,d\mathbf{k}'\right] \delta f\,d\mathbf{k}\,dt \\
&+ \int_{\mathbb{R}^2} [\varphi(\mathbf{k}) + q(T,\mathbf{k})]\,\delta f(T,\mathbf{k})\,d\mathbf{k}.
\end{aligned}
$$

Thus by requiring $(\nabla_f \mathcal{L}, \delta f) = 0$ for all possible variations δf, we obtain the adjoint equation

$$
\begin{aligned}
&- \partial_t q(t,\mathbf{k}) - \mathbf{u}\cdot\nabla_{\mathbf{k}} q(t,\mathbf{k}) - \int_{\mathbb{R}^2} S(\mathbf{k}',\mathbf{k}) f(\mathbf{k}')(q(t,\mathbf{k}') - q(t,\mathbf{k}))\,d\mathbf{k}' \\
&- \int_{\mathbb{R}^2} S(\mathbf{k},\mathbf{k}')(1-f(\mathbf{k}'))(q(t,\mathbf{k}') - q(t,\mathbf{k}))\,d\mathbf{k}' + \theta(t,\mathbf{k}) = 0,
\end{aligned}
$$

or equivalently

$$
-\partial_t q(t,\mathbf{k}) - \mathbf{u}\cdot\nabla_{\mathbf{k}} q(t,\mathbf{k}) - C^*[f,q](t,\mathbf{k}) + \theta(t,\mathbf{k}) = 0,
$$

where we have defined

$$
\begin{aligned}
C^*[f,q](t,\mathbf{k}) &= \int_{\mathbb{R}^2} S(\mathbf{k}',\mathbf{k}) f(\mathbf{k}')(q(t,\mathbf{k}') - q(t,\mathbf{k}))\,d\mathbf{k}' \\
&+ \int_{\mathbb{R}^2} S(\mathbf{k},\mathbf{k}')(1-f(\mathbf{k}'))(q(t,\mathbf{k}') - q(t,\mathbf{k}))\,d\mathbf{k}'.
\end{aligned}
$$

Furthermore, considering the term with the variation at final time, we obtain the terminal condition $q(T,\mathbf{k}) = -\varphi(\mathbf{k})$.

Now, we collect our equations that form the optimality system:

$$\begin{aligned} &\partial_t f + \mathbf{u}\cdot\nabla_{\mathbf{k}} f = C[f,f], && f(0)=f_0 \\ &-\partial_t q - \mathbf{u}\cdot\nabla_{\mathbf{k}} q = C^*[f,q] - \theta, && q(T) = -\varphi, \\ &\nu\,\mathbf{u} - \nu\,\mathbf{u}'' + \int_{\mathbb{R}^2} q\nabla_{\mathbf{k}} f\, d\mathbf{k} = \mathbf{0}, && \mathbf{u}(0)=\mathbf{0},\ \mathbf{u}(T)=\mathbf{0}. \end{aligned} \tag{4.4}$$

5. Discontinuous Galerkin approximation

In this section, we discuss the numerical approximation of the optimality system (4.4) by means of a discontinuous Galerkin (DG) method. Specifically, we develop a first-order DG method with a second-order Runge–Kutta time-integration scheme; see, e.g., [32].

Based on the statement of Theorem 1, we can assume that choosing an initial condition with sufficiently fast decay to zero as $|\mathbf{k}| \to +\infty$, we can expect a solution f with similar decay, thus making reasonable to consider our optimality system defined on a bounded convex domain $\Omega \subseteq \mathbb{R}^2$, such that $f(t,\mathbf{k}) \approx 0$ for $\mathbf{k} \in \partial\Omega$ and $t \geq 0$. Further, we assume that the setting of our optimal control problem is such that $q(t,\mathbf{k}) \approx 0$ for $\mathbf{k} \in \partial\Omega$ and $t \geq 0$.

Specifically, we choose Ω equal to a disk centered at $(0,0)$ and radius k^2_{max}, and take f_0, θ and φ such that the assumption of homogeneous boundary conditions for f and q are met.

Now, we introduce a finite decomposition $\{C_\alpha : \alpha = 1,2,\dots,N\}$ of the domain Ω as follows:

$$C_\alpha \subseteq \Omega, \quad C_\alpha \cap C_\beta = \emptyset, \quad \alpha \neq \beta, \quad \bigcup_{\alpha=1}^{N} \overline{C}_\alpha = \Omega.$$

We adopt polar coordinates:

$$\begin{cases} k_x = \sqrt{s}\cos\vartheta \\ k_y = \sqrt{s}\sin\vartheta \end{cases} \tag{5.1}$$

with $(s,\vartheta) \in [0, s_{max}] \times [0, 2\pi]$, and the cell C_α is given by

$$\overline{C}_\alpha = \left\{ (s,\vartheta) \in [0,s_{max}] \times [0,2\pi] \ :\ s_{k-\frac{1}{2}} \leq s \leq s_{k+\frac{1}{2}},\ \vartheta_{n-\frac{1}{2}} \leq \vartheta \leq \vartheta_{n+\frac{1}{2}} \right\}, \tag{5.2}$$

where $s_{max} = k^2_{max}$, with subintervals of size $\Delta s = s_{max}/N_s$ that are centered at $s_k = \Delta s\,(k-1/2)$, $k = 1,2,\dots,N_s$. Similarly, we have $\Delta\vartheta = 2\pi/N_\vartheta$, $\vartheta_n = \Delta\vartheta\,(n-1/2)$, $n = 1,2,\dots,N_\vartheta$.

We remark that the basis vectors in the Cartesian coordinates (k_x,k_y) and in the polar one satisfy the relations

$$\begin{cases} \hat{\mathbf{e}}_{k_x} = \cos\vartheta\,\hat{\mathbf{e}}_s - \sin\vartheta\,\hat{\mathbf{e}}_\vartheta \\ \hat{\mathbf{e}}_{k_y} = \sin\vartheta\,\hat{\mathbf{e}}_s + \cos\vartheta\,\hat{\mathbf{e}}_\vartheta \end{cases} \tag{5.3}$$

thus for the gradients we have

$$\nabla_{\mathbf{k}} = \hat{\mathbf{e}}_s \left(2\sqrt{s}\,\frac{\partial}{\partial s} \right) + \hat{\mathbf{e}}_\vartheta \left(\frac{1}{\sqrt{s}}\,\frac{\partial}{\partial\vartheta} \right). \tag{5.4}$$

We assume a constant approximation for the functions f and q in each cell C_α. By introducing the characteristic function χ_α on the cell C_α, we can write

$$f(t,\mathbf{k}) \approx \sum_{\alpha=1}^{N} f^\alpha(t)\,\chi_\alpha(\mathbf{k}), \qquad q(t,\mathbf{k}) \approx \sum_{\alpha=1}^{N} q^\alpha(t)\,\chi_\alpha(\mathbf{k}).$$

Based on this piecewise constant approximation, we derive a set of ordinary differential equations governing the time evolution of $f^\alpha(t)$ and $q^\alpha(t)$. For this purpose, we integrate our Boltzmann equation and its adjoint over the cell C_α. We have

$$\int_{C_\alpha} \partial_t f\, d\mathbf{k} + \int_{C_\alpha} \mathbf{u}\cdot\nabla_{\mathbf{k}} f\, d\mathbf{k} = \int_{C_\alpha} C[f,f]\, d\mathbf{k}, \tag{5.5}$$

$$-\int_{C_\alpha} \partial_t q\, d\mathbf{k} - \int_{C_\alpha} \mathbf{u}\cdot\nabla_{\mathbf{k}} q\, d\mathbf{k} - \int_{C_\alpha} C^*[f,q]\, d\mathbf{k} + \int_{C_\alpha} \theta(t,\mathbf{k})\, d\mathbf{k} = 0. \tag{5.6}$$

The integrals of the terms containing time derivatives give

$$\int_{C_\alpha} \partial_t f(t,\mathbf{k})\, d\mathbf{k} \approx M_\alpha\, \frac{df^\alpha}{dt}(t), \qquad \int_{C_\alpha} \partial_t q(t,\mathbf{k})\, d\mathbf{k} \approx M_\alpha\, \frac{dq^\alpha}{dt}(t),$$

where M_α is the area of the cell C_α.

The integrals involving the control and gradients of f and q are transformed by using Gauss' theorem:

$$\mathbf{u}(t)\cdot\int_{C_\alpha}\nabla_{\mathbf{k}} f\, d\mathbf{k} = \mathbf{u}(t)\cdot\int_{\partial C_\alpha} f\,\mathbf{n}\,ds, \qquad \text{and} \qquad -\mathbf{u}(t)\cdot\int_{C_\alpha}\nabla_{\mathbf{k}} q\, d\mathbf{k} = -\mathbf{u}(t)\cdot\int_{\partial C_\alpha} q\,\mathbf{n}\,ds,$$

where we estimate f and q on the boundary of the cells by a standard reconstruction procedure based on a min-mod slope limiter [8].

Next, we discuss the treatment of the terms arising from the collision operator. For $\mathbf{k}\in C_\alpha$, we have

$$\begin{aligned} C[f,f](t,\mathbf{k}) &= (1-f(t,\mathbf{k}))\int_{\mathbb{R}^2} S(\mathbf{k},\mathbf{k}')\, f(t,\mathbf{k}')\, d\mathbf{k}' - f(t,\mathbf{k})\int_{\mathbb{R}^2} S(\mathbf{k}',\mathbf{k})\left(1-f(t,\mathbf{k}')\right) d\mathbf{k}' \\ &\approx \sum_{\beta=1}^{N}\left[(1-f^\alpha(t))\int_{C_\beta} S(\mathbf{k},\mathbf{k}')\, f(t,\mathbf{k}')\, d\mathbf{k}' - f^\alpha(t)\int_{C_\beta} S(\mathbf{k}',\mathbf{k})\left(1-f(t,\mathbf{k}')\right) d\mathbf{k}'\right] \\ &\approx \sum_{\beta=1}^{N}\left[(1-f^\alpha(t))\, f^\beta(t)\int_{C_\beta} S(\mathbf{k},\mathbf{k}')\, d\mathbf{k}' - f^\alpha(t)\left(1-f^\beta(t)\right)\int_{C_\beta} S(\mathbf{k},\mathbf{k}')\, d\mathbf{k}'\right]. \end{aligned}$$

So, defining

$$A^{\alpha,\beta} = \int_{C_\alpha}\left[\int_{C_\beta} S(\mathbf{k}',\mathbf{k})\, d\mathbf{k}'\right] d\mathbf{k}, \tag{5.7}$$

it follows that

$$\int_{C_\alpha} C[f,f]\, d\mathbf{k} \approx \sum_{\beta=1}^{N}\left[A^{\beta,\alpha}\,(1-f^\alpha(t))\, f^\beta(t) - A^{\alpha,\beta}\, f^\alpha(t)(1-f^\beta(t))\right]. \tag{5.8}$$

Analogously, for the collision term of the adjoint equation, we get

$$\int_{C_\alpha} C^*[f,q]\, d\mathbf{k} \approx \sum_{\beta=1}^{N}\left[A^{\beta,\alpha} f^\beta(t)(q^\beta(t)-q^\alpha(t)) + A^{\alpha,\beta}\,(1-f^\beta(t))(q^\beta(t)-q^\alpha(t))\right]. \tag{5.9}$$

Finally, we adopt the same approach for the tracking term and we obtain

$$\int_{C_\alpha} \theta(t,\mathbf{k})\, d\mathbf{k} \approx M_\alpha \theta^\alpha(t). \tag{5.10}$$

Moreover, following the approach in [8], we obtain the discretization of the forward equation as follows:

$$\begin{aligned} \frac{\Delta s\Delta\vartheta}{2}\frac{d}{dt} f^{(k,n)}(t) = &-(\mathbf{u}(t)\cdot\mathbf{i})\left\{\left[\sqrt{s_{k+\frac12}}\,\tilde f_{k+\frac12,n} - \sqrt{s_{k-\frac12}}\,\tilde f_{k-\frac12,n}\right]\int_{\vartheta_{n-\frac12}}^{\vartheta_{n+\frac12}}\cos\vartheta\, d\vartheta\right. \\ &\left. - \left[\sin\vartheta_{n+\frac12}\tilde f_{k,n+\frac12} - \sin\vartheta_{n-\frac12}\tilde f_{k,n-\frac12}\right]\int_{s_{k-\frac12}}^{s_{k+\frac12}}\frac{1}{2\sqrt{s}}\, ds\right\} \\ &-(\mathbf{u}(t)\cdot\mathbf{j})\left\{\left[\sqrt{s_{k+\frac12}}\,\tilde f_{k+\frac12,n} - \sqrt{s_{k-\frac12}}\,\tilde f_{k-\frac12,n}\right]\int_{\vartheta_{n-\frac12}}^{\vartheta_{n+\frac12}}\sin\vartheta\, d\vartheta\right. \\ &\left. + \left[\cos\vartheta_{n+\frac12}\tilde f_{k,n+\frac12} - \cos\vartheta_{n-\frac12}\tilde f_{k,n-\frac12}\right]\int_{s_{k-\frac12}}^{s_{k+\frac12}}\frac{1}{2\sqrt{s}}\, ds\right\} \\ &+\sum_{k'=1}^{N_s}\sum_{n'=1}^{N_\vartheta}\left[A^{(k',n'),(k,n)}\left(1-f^{(k,n)}(t)\right) f^{(k',n')}(t)\right. \\ &\left. -A^{(k,n),(k',n')} f^{(k,n)}(t)\left(1-f^{(k',n')}(t)\right)\right], \end{aligned} \tag{5.11}$$

where $\tilde f$ represents a numerical flux function which provides an approximation of f at the boundary of the cell.

Similarly, after a time reversion, the discretization of the adjoint equation writes

$$\begin{aligned}
\frac{\Delta s \Delta \vartheta}{2}\frac{d}{dt}q^{(k,n)}(t) = (\mathbf{u}(t)\cdot\mathbf{i})&\Bigg\{\left[\sqrt{s_{k+\frac{1}{2}}}\tilde{q}_{k+\frac{1}{2},n} - \sqrt{s_{k-\frac{1}{2}}}\tilde{q}_{k-\frac{1}{2},n}\right]\int_{\vartheta_{n-\frac{1}{2}}}^{\vartheta_{n+\frac{1}{2}}}\cos\vartheta\, d\vartheta \\
&- \left[\sin\vartheta_{n+\frac{1}{2}}\tilde{q}_{k,n+\frac{1}{2}} - \sin\vartheta_{n-\frac{1}{2}}\tilde{q}_{k,n-\frac{1}{2}}\right]\int_{s_{k-\frac{1}{2}}}^{s_{k+\frac{1}{2}}}\frac{1}{2\sqrt{s}}\, ds\Bigg\} \\
&+ (\mathbf{u}(t)\cdot\mathbf{j})\Bigg\{\left[\sqrt{s_{k+\frac{1}{2}}}\tilde{q}_{k+\frac{1}{2},n} - \sqrt{s_{k-\frac{1}{2}}}\tilde{q}_{k-\frac{1}{2},n}\right]\int_{\vartheta_{n-\frac{1}{2}}}^{\vartheta_{n+\frac{1}{2}}}\sin\vartheta\, d\vartheta \\
&+ \left[\cos\vartheta_{n+\frac{1}{2}}\tilde{q}_{k,n+\frac{1}{2}} - \cos\vartheta_{n-\frac{1}{2}}\tilde{q}_{k,n-\frac{1}{2}}\right]\int_{s_{k-\frac{1}{2}}}^{s_{k+\frac{1}{2}}}\frac{1}{2\sqrt{s}}\, ds\Bigg\} \\
&+ \sum_{k'=1}^{N_s}\sum_{n'=1}^{N_\vartheta}\Big[A^{(k',n'),(k,n)} f^{(k',n')}(t)(q^{(k',n')}(t) - q^{(k,n)}(t)) \\
&+ A^{(k,n),(k',n')}(1 - f^{(k',n')}(t))(q^{(k',n')}(t) - q^{(k,n)}(t))\Big] \\
&- \frac{\Delta s \Delta \vartheta}{2}\theta^{(k,n)}(t),
\end{aligned} \tag{5.12}$$

where $\tilde{q}$ represents a numerical flux function which provides an approximation of f at the boundary of the cell.

The same discretization can be adopted to compute the following macroscopic quantities

$$n(t) \approx \frac{2}{(2\pi)^2}\sum_{k=1}^{N_s}\sum_{n=1}^{N_\theta} f^{(k,n)}(t) \tag{5.13}$$

$$\langle\mathbf{k}\rangle(t) \approx \frac{2}{(2\pi)^2}\frac{1}{2}\frac{1}{n(t)}\sum_{k=1}^{N_s}\sum_{n=1}^{N_\theta} f^{(k,n)}(t)\int_{s_{k-\frac{1}{2}}}^{s_{k+\frac{1}{2}}}\sqrt{s}\, ds\int_{\theta_{n-\frac{1}{2}}}^{\theta_{n+\frac{1}{2}}}(\cos\theta, \sin\theta)\, d\theta \tag{5.14}$$

$$\langle\mathbf{v}\rangle(t) \approx \frac{2}{(2\pi)^2}\frac{v_F \Delta s}{2}\frac{1}{n(t)}\sum_{k=1}^{N_s}\sum_{n=1}^{N_\theta} f^{(k,n)}(t)\int_{\theta_{n-\frac{1}{2}}}^{\theta_{n+\frac{1}{2}}}(\cos\theta, \sin\theta)\, d\theta \tag{5.15}$$

$$\langle\varepsilon\rangle(t) \approx \frac{2}{(2\pi)^2}\frac{\hbar v_F \Delta\theta}{2}\frac{1}{n(t)}\sum_{k=1}^{N_s}\sum_{n=1}^{N_\theta} f^{(k,n)}(t)\int_{s_{k-\frac{1}{2}}}^{s_{k+\frac{1}{2}}}\sqrt{s}\, ds. \tag{5.16}$$

6. Numerical optimization

Our approach for solving the Boltzmann optimal control problem (4.4) is based on the nonlinear conjugate gradient (NCG) method; see, e.g., [1]. This is an iterative method that resembles the standard CG scheme and requires to estimate the reduced gradient $\nabla_{\mathbf{u}} J_r$ at each iteration.

In order to illustrate the NCG method, we start with a preliminary discussion on the construction of the gradient. For a given $\mathbf{u}$ obtained after a number of iterations, we sequentially solve the Boltzmann equation and its adjoint, and use (4.3) to assemble the L^2 gradient. However, since the control is sought in $H^1(0,T;\mathbb{R}^2)$, we need to obtain the H^1 gradient that satisfies the following relation

$$\left(\nabla J_r(\mathbf{u})|_{H^1}, \delta\mathbf{u}\right)_{H^1} = \left(\nabla J_r(\mathbf{u})|_{L^2}, \delta\mathbf{u}\right)_{L^2}. \tag{6.1}$$

Now, using the definition of the H^1 inner product, we obtain

$$\int_0^T\left[\nabla J_r(\mathbf{u})|_{H^1}\cdot\delta\mathbf{u}(t) + \frac{d}{dt}\nabla J_r(\mathbf{u})|_{H^1}\cdot\delta\mathbf{u}'(t)\right]dt = \int_0^T \nabla J_r(\mathbf{u})|_{L^2}\cdot\delta\mathbf{u}(t)\, dt, \tag{6.2}$$

which must hold for all the test functions $\delta\mathbf{u} \in H_0^1(0,T)$. Therefore we obtain

$$-\frac{d^2}{dt^2}\left[\nabla J_r(\mathbf{u})|_{H^1}\right] + \left[\nabla J_r(\mathbf{u})|_{H^1}\right] = \nabla J_r(\mathbf{u})|_{L^2}, \tag{6.3}$$

with the conditions $\nabla J_r(\mathbf{u})|_{H^1}(0) = \mathbf{0}$ and $\nabla J_r(\mathbf{u})|_{H^1}(T) = \mathbf{0}$. We approximate (6.3) by standard finite differences on the interval $(0,T)$, which results in a tridiagonal linear system that is efficiently solved by the Thomas' algorithm.

Now, we give details on the assembly of the L^2 gradient (4.3). The main effort is the computation of the integral in this formula using our modified polar coordinates. We also consider a finite differences approximation of $[0,T]$ on the grid with points $t^i = i\,\Delta t$,

$i = 0, \dots, N_t$, $\Delta t = T/N_t$, therefore we denote by $f^{i,k,n}$ and $q^{i,k,n}$ the approximation of $f(t,\mathbf{k})$ and $q(t,\mathbf{k})$ in $[t_{i-1}, t_i] \times C_\alpha$. Hence, we have

$$
\begin{aligned}
I_{gr} = (I^1_{gr}, I^2_{gr}) &:= \int_{\mathbb{R}^2} q(t,\mathbf{k}) \nabla_{\mathbf{k}} f(t,\mathbf{k})\, d\mathbf{k} \\
&= \int_0^{2\pi}\int_0^{+\infty} \frac{1}{2} q(t,s,\vartheta) \left[\hat{\mathbf{e}}_s \left(2\sqrt{s} \frac{\partial f(t,s,\vartheta)}{\partial s} \right) + \hat{\mathbf{e}}_\vartheta \left(\frac{\sqrt{s}}{s} \frac{\partial f(t,s,\vartheta)}{\partial \vartheta} \right) \right] ds\, d\vartheta \\
&= \int_0^{2\pi}\int_0^{+\infty} q(t,s,\vartheta) \left[\left(\sqrt{s} \cos\vartheta \frac{\partial f(t,s,\vartheta)}{\partial s} - \frac{1}{2\sqrt{s}} \sin\theta \frac{\partial f(t,s,\vartheta)}{\partial \vartheta} \right) \mathbf{i} \right. \\
&\left. + \left(\sqrt{s} \sin\vartheta \frac{\partial f(t,s,\vartheta)}{\partial s} + \frac{1}{2\sqrt{s}} \cos\theta \frac{\partial f(t,s,\vartheta)}{\partial \vartheta} \right) \mathbf{j} \right] ds\, d\vartheta \\
&= \int_0^{2\pi}\int_0^{+\infty} q(t,s,\vartheta) \left[\frac{\partial}{\partial s} \left(\sqrt{s} \cos\vartheta f(t,s,\vartheta) \right) - \frac{\partial}{\partial \vartheta} \left(\frac{1}{2\sqrt{s}} \sin\vartheta f(t,s,\vartheta) \right) \right] \mathbf{i}\, ds\, d\vartheta \\
&+ \int_0^{2\pi}\int_0^{+\infty} q(t,s,\vartheta) \left[\frac{\partial}{\partial s} \left(\sqrt{s} \sin\vartheta f(t,s,\vartheta) \right) + \frac{\partial}{\partial \vartheta} \left(\frac{1}{2\sqrt{s}} \cos\vartheta f(t,s,\vartheta) \right) \right] \mathbf{j}\, ds\, d\vartheta \\
&\approx \sum_{k=1}^{N_s}\sum_{n=1}^{N_\vartheta} q^{i,k,n} \left[\int_{\vartheta_{n-\frac{1}{2}}}^{\vartheta_{n+\frac{1}{2}}} \left[\sqrt{s} \cos\vartheta f(t,s,\vartheta) \right]_{s_{k-\frac{1}{2}}}^{s_{k+\frac{1}{2}}} d\vartheta - \int_{s_{k-\frac{1}{2}}}^{s_{k+\frac{1}{2}}} \left[\frac{1}{2\sqrt{s}} \sin\vartheta f(t,s,\vartheta) \right]_{\vartheta_{n-\frac{1}{2}}}^{\vartheta_{n+\frac{1}{2}}} ds \right] \mathbf{i} \\
&+ \sum_{k=1}^{N_s}\sum_{n=1}^{N_\vartheta} q^{i,k,n} \left[\int_{\vartheta_{n-\frac{1}{2}}}^{\vartheta_{n+\frac{1}{2}}} \left[\sqrt{s} \sin\vartheta f(t,s,\vartheta) \right]_{s_{k-\frac{1}{2}}}^{s_{k+\frac{1}{2}}} d\vartheta + \int_{s_{k-\frac{1}{2}}}^{s_{k+\frac{1}{2}}} \left[\frac{1}{2\sqrt{s}} \cos\vartheta f(t,s,\vartheta) \right]_{\vartheta_{n-\frac{1}{2}}}^{\vartheta_{n+\frac{1}{2}}} ds \right] \mathbf{j} \\
&\approx \sum_{k=1}^{N_s}\sum_{n=1}^{N_\vartheta} q^{i,k,n} \left[\left(\sqrt{s_{k+\frac{1}{2}}} f^{i,k+\frac{1}{2},n} - \sqrt{s_{k-\frac{1}{2}}} f^{i,k-\frac{1}{2},n} \right) \int_{\vartheta_{n-\frac{1}{2}}}^{\vartheta_{n+\frac{1}{2}}} \cos\vartheta\, d\vartheta \right. \\
&\left. - \left(\sin\vartheta_{n+\frac{1}{2}} f^{i,k,n+\frac{1}{2}} - \sin\vartheta_{n+\frac{1}{2}} f^{i,k,n-\frac{1}{2}} \right) \int_{s_{k-\frac{1}{2}}}^{s_{k+\frac{1}{2}}} \frac{1}{2\sqrt{s}}\, ds \right] \mathbf{i} \\
&+ \sum_{k=1}^{N_s}\sum_{n=1}^{N_\vartheta} q^{i,k,n} \left[\left(\sqrt{s_{k+\frac{1}{2}}} f^{i,k+\frac{1}{2},n} - \sqrt{s_{k-\frac{1}{2}}} f^{i,k-\frac{1}{2},n} \right) \int_{\vartheta_{n-\frac{1}{2}}}^{\vartheta_{n+\frac{1}{2}}} \sin\vartheta\, d\vartheta \right. \\
&\left. + \left(\cos\vartheta_{n+\frac{1}{2}} f^{i,k,n+\frac{1}{2}} - \cos\vartheta_{n+\frac{1}{2}} f^{i,k,n-\frac{1}{2}} \right) \int_{s_{k-\frac{1}{2}}}^{s_{k+\frac{1}{2}}} \frac{1}{2\sqrt{s}}\, ds \right] \mathbf{j}.
\end{aligned}
$$

Since f is not defined on the boundary of the cells, we adopt a linear interpolation formula, that is,

$$
\begin{aligned}
f^{i,k\pm\frac{1}{2},n} &\approx \frac{1}{2}\left(f^{i,k+\frac{1}{2}\pm\frac{1}{2},n} + f^{i,k-\frac{1}{2}\pm\frac{1}{2},n} \right), \qquad k = 2,3,\dots,N_s-1, \quad n = 1,2,\dots,N_\vartheta, \\
f^{i,k,n\pm\frac{1}{2}} &\approx \frac{1}{2}\left(f^{i,k,n+\frac{1}{2}\pm\frac{1}{2}} + f^{i,k,n-\frac{1}{2}\pm\frac{1}{2}} \right), \qquad k = 1,2,\dots,N_s, \quad n = 2,3,\dots,N_\vartheta-1.
\end{aligned}
$$

Moreover, we adopt zero flux extension in the s direction,

$$
\begin{aligned}
f^{i,\frac{1}{2},n} &= f^{i,1,n}, \qquad n = 1,2,\dots,N_\vartheta, \\
f^{i,N_s+\frac{1}{2},n} &= f^{i,N_s,n}, \qquad n = 1,2,\dots,N_\vartheta,
\end{aligned}
$$

and periodic extension in the ϑ direction,

$$
f^{i,k,\frac{1}{2}} = f^{i,k,N_\vartheta+\frac{1}{2}} \approx \frac{1}{2}\left(f^{i,k,1} + f^{i,k,N_\vartheta} \right), \qquad k = 1,2,\dots,N_s.
$$

With this preparation, we can present the numerical approximation of the L^2 reduced gradient at $\mathbf{u} = (u_x, u_y)$ as a two-component function on the time interval $[0,T]$, is given by

$$
\begin{aligned}
\nabla_{\mathbf{u}} J_r|^1_{L^2}(t^i) &= \nu u^i_x - \frac{\nu}{\Delta t^2}(u^{i-1}_x - 2u^i_x + u^{i+1}_x) + I^1_{gr}, \\
\nabla_{\mathbf{u}} J_r|^2_{L^2}(t^i) &= \nu u^i_y - \frac{\nu}{\Delta t^2}(u^{i-1}_y - 2u^i_y + u^{i+1}_y) + I^2_{gr},
\end{aligned}
\tag{6.4}
$$

where $i = 1,2,\dots,N_t-1$, and $\nabla_{\mathbf{u}} J_r|^1_{L^2}(0) = 0$, $\nabla_{\mathbf{u}} J_r|^1_{L^2}(T) = 0$, $\nabla_{\mathbf{u}} J_r|^2_{L^2}(0) = 0$, and $\nabla_{\mathbf{u}} J_r|^2_{L^2}(T) = 0$.

Next, we summarize in Algorithm 6.1 our procedure for computing the gradient.

Algorithm 6.1 Calculate H^1 reduced gradient.

Require: control $\mathbf{u}(t)$, $f_0(\mathbf{k})$, $\varphi(\mathbf{k})$, $\theta(\mathbf{k},t)$
Ensure: reduced gradient $\nabla J_r(\mathbf{u})|_{H^1}$
Solve forward equation by the DG method with inputs: $f_0(\mathbf{k})$, $\mathbf{u}(t)$
Solve backward equation by the DG method with inputs: $\varphi(\mathbf{k})$, $\mathbf{u}(t)$, $\theta(\mathbf{k},t)$
Assemble the L^2 reduced gradient $\nabla J_r(\mathbf{u})|_{L^2}$ using (6.4).
Compute the H^1 reduced gradient $\nabla J_r(\mathbf{u})|_{H^1}$ solving (6.3).
return $\nabla J_r(\mathbf{u})|_{H^1}$

Now, we can discuss the NCG method given in Algorithm 6.2. We initialize the NCG iterative procedure with $\mathbf{u}^0(t) = \mathbf{0}$. We denote the optimization directions with $\mathbf{d}^n$. In the first update, we have $\mathbf{d}^0 = -\nabla J_r(\mathbf{u}^0)|_{H^1}$ and perform the optimization step

$$\mathbf{u}^1 = \mathbf{u}^0 + \alpha_0\, \mathbf{d}^0,$$

where α_0 is obtained by a backtracking linesearch procedure. After the first step, in the NCG method the descent direction is defined as a linear combination of the new gradient and the past direction as follows:

$$\mathbf{d}^n = -\nabla J_r(\mathbf{u}^n)|_{H^1} + \beta_{n-1}\, \mathbf{d}^{n-1},$$

where $\beta_{-1} = 0$, and $\beta_{n-1} = \|\nabla J_r(\mathbf{u}^n)|_{H^1}\|^2 / \|\nabla J_r(\mathbf{u}^{n-1})|_{H^1}\|^2$, that is, the Fletcher–Reeves formula; however, other choices are possible [33].

The tolerance *tol* and the maximum number of iterations $n_{\max}$ are used for termination criteria. Summarizing, we have the following NCG algorithm.

Algorithm 6.2 Nonlinear conjugate gradient (NCG) method

Require: $u^0(t)$, $f_0(\mathbf{k})$, $\varphi(\mathbf{k})$, $\theta(t,\mathbf{k})$
Ensure: Optimal control $\mathbf{u}(t)$ and corresponding state $f(t,\mathbf{k})$
$n = 0$
Assemble gradient $\mathbf{g}^0 = \nabla J_r(\mathbf{u}^0)|_{H^1}$ using Algorithm 6.1; set $\mathbf{d}^0 = -\mathbf{g}^0$.
while $\|\mathbf{g}^n\|_{H^1_T} > tol$ **and** $n < n_{\max}$ **do**
  Use linesearch to determine α_n
  Update control: $\mathbf{u}^{n+1} = \mathbf{u}^n + \alpha_n \mathbf{d}^n$
  Compute the gradient $\mathbf{g}^{n+1} = \nabla J_r(\mathbf{u}^{n+1})|_{H^1}$ using Algorithm 6.1
  Calculate the new descent direction $\mathbf{d}^{n+1} = -\mathbf{g}^{n+1} + \beta_n\, \mathbf{d}^n$
  Set $n = n + 1$
end while
return $(\mathbf{u}^n, f^n)$

7. Numerical experiments

In this section, we present results of numerical experiments that validate the ability of our optimal control framework to steer the ensemble of electrons to follow in the mean a given trajectory configuration in the wave-vector space. Similarly, we show how to apply our framework to manipulate the current density.

We present results of different experiments with various desired trajectories denoted with $\mathbf{k}_d(t)$, and compute the corresponding optimal control $\mathbf{u}$. For all numerical experiments, we choose the values of the simulation parameters $N_s = 1200$, $N_\vartheta = 64$, and $N_t = 600$.

Our first experiment considers $\mathbf{k}_d(t)$ given by

$$(\mathbf{k}_d(t))_x = (\mathbf{k}_d(t))_y = \begin{cases} 2\dfrac{t}{T}\tilde{k} & \text{if} \quad 0 \le t \le \dfrac{T}{2} \\ 2\left(1 - \dfrac{t}{T}\right)\tilde{k} & \text{if} \quad \dfrac{T}{2} \le t \le T \end{cases} \tag{7.1}$$

For the test we choose $T = 3$ ps, $\tilde{k} = 0.1$ nm^{-1}. Notice that $\mathbf{k}_d(t)$ represents a continuous trajectory with a point of discontinuity in the first derivative.

The results of this experiment are depicted in the Figs. 1–4. In particular, in Fig. 1 we plot the mean values of the wave-vector, that is, $\langle\mathbf{k}\rangle(t)$, versus time and the desired trajectory $\mathbf{k}_d(t)$. In Fig. 2, the time behaviors of the two components of the computed optimal electric control field are plotted. In Figs. 3 and 4 the corresponding mean values of velocity and energy are presented.

We remark that our choice of a H^1 regularization of the control function was motivated by the modeling requirement of a guaranteed continuous optimal control that can be switched on and off at the endpoints of the time interval, and we have also used the continuity property of $\mathbf{u}$ in our analytical investigation in the proof of Theorem 1. However, for completeness we would like to illustrate results of a similar optimal control problem where the cost term $\frac{\nu}{2}\|\mathbf{u}\|^2_{H^1(0,T)}$ in (4.2) is replaced by $\frac{\nu}{2}\|\mathbf{u}\|^2_{L^2(0,T)}$. We

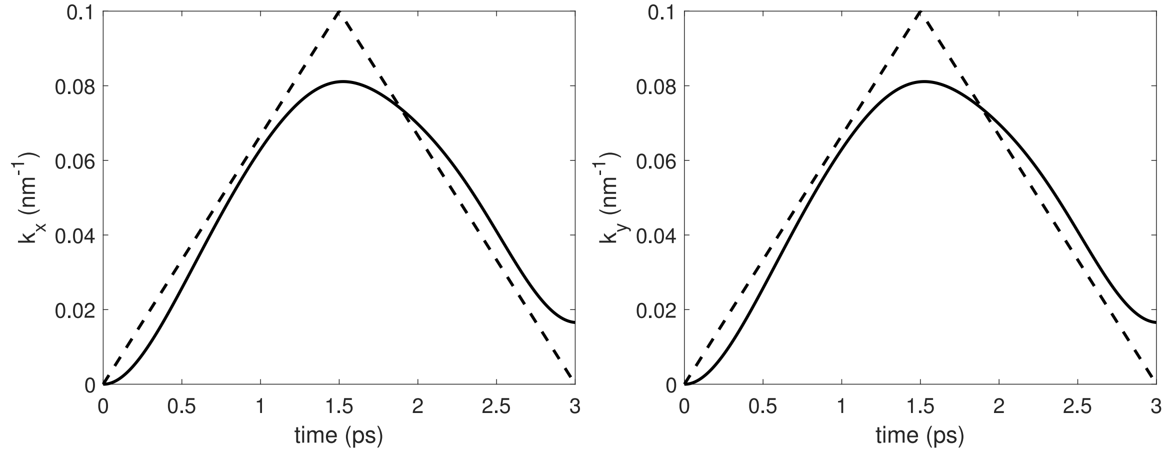

Fig. 1. Computed mean values $\langle \mathbf{k} \rangle$ (continuous line) and desired trajectory $\mathbf{k}_d$ (dashed line) versus time in the case of the desired trajectory given by (7.1); x (left) and y components.

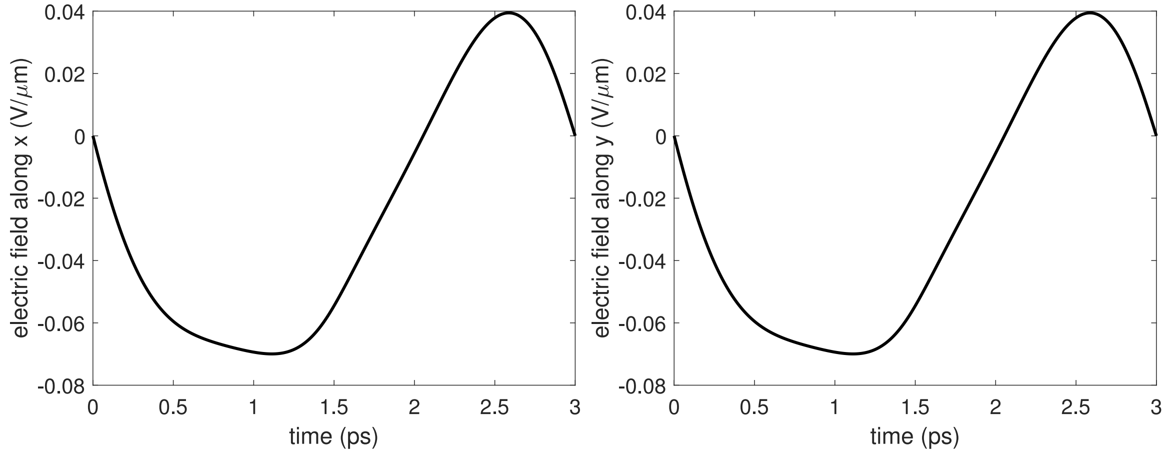

Fig. 2. Optimal electric control field versus time in the case of the desired trajectory given by (7.1); x and y components.

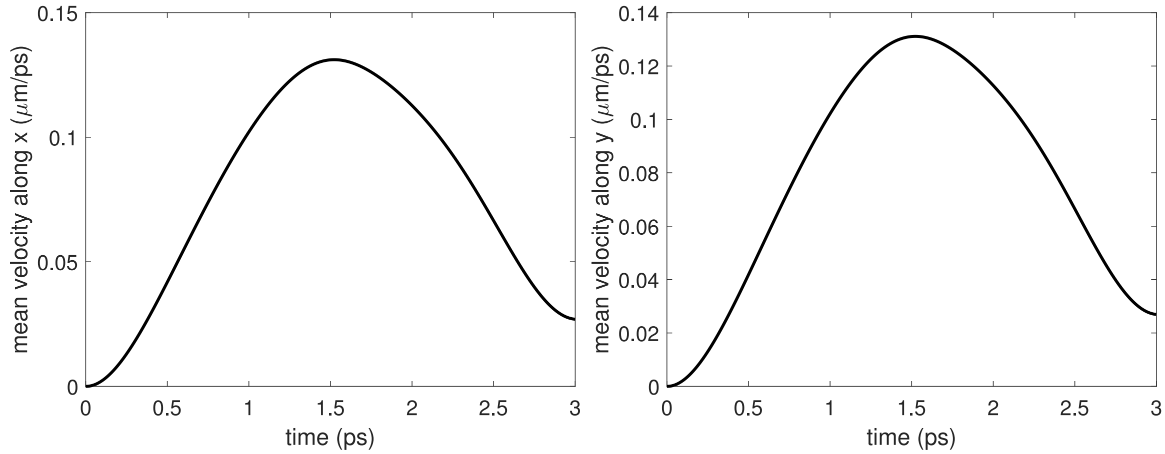

Fig. 3. Mean values of the velocity versus time in the case of the desired trajectory given by (7.1); x and y components.

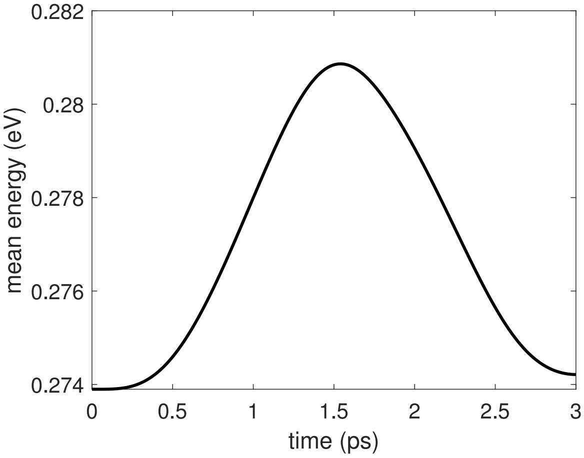

Fig. 4. Mean values of the energy versus time in the case of the desired trajectory given by (7.1).

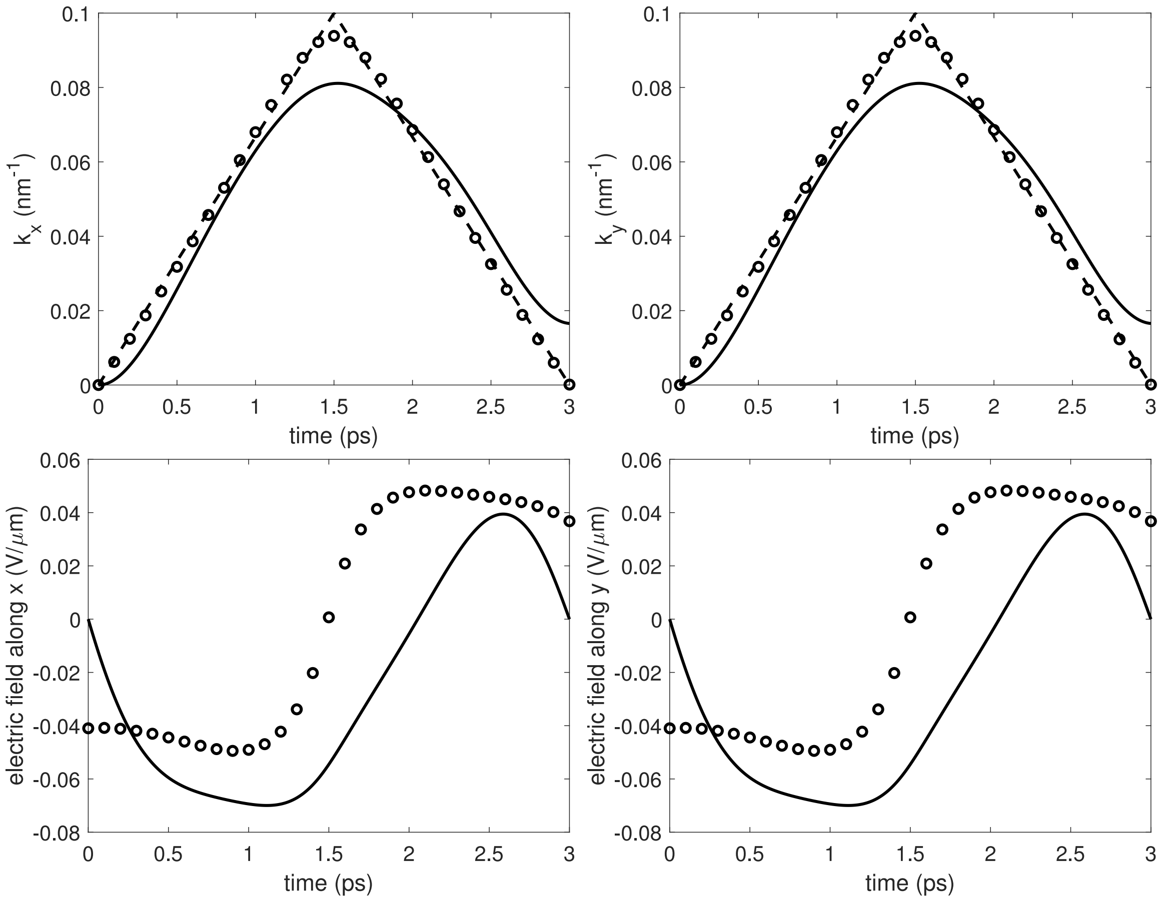

Fig. 5. Computed mean values $\langle \mathbf{k} \rangle$ corresponding to optimal H^1 controls (continuous line) and to L^2 controls (dotted-circle line), and the desired trajectory $\mathbf{k}_d$ (dashed line) versus time.

compare the results obtained in these two cases in Fig. 5. Clearly, the latter is a larger space, which gives the possibility to attain better tracking results as it can be seen in the figure. On the other hand, in the L^2 case, we have no way to fix the value of the control at initial and final time, and in principle highly discontinuous controls might result. These facts are also visible in Fig. 5, where the optimal L^2 control shows much steeper changes in time.

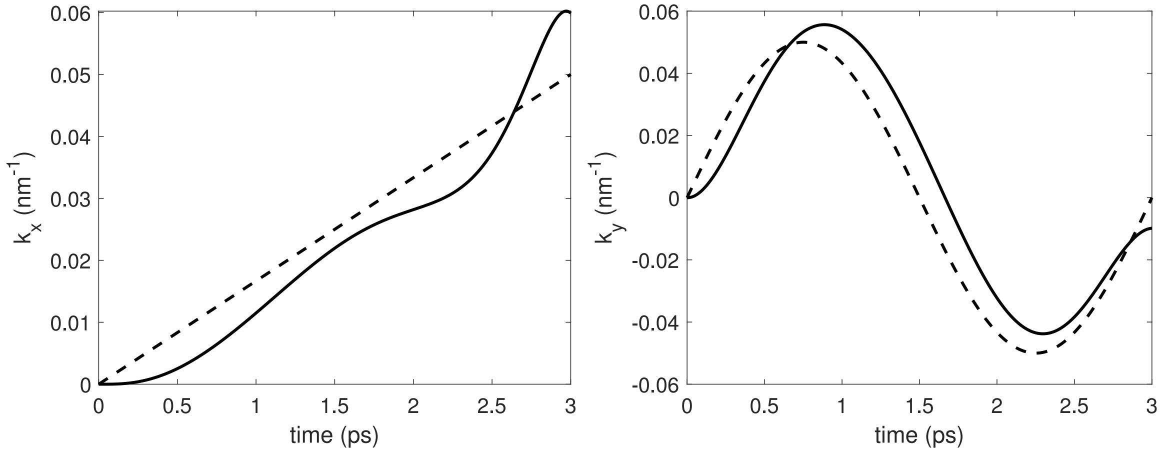

Fig. 6. Computed mean values $\langle \mathbf{k} \rangle$ (continuous line) and desired trajectory $\mathbf{k}_d$ (dashed line) versus time in the case of the desired trajectory given by (7.2); x (left) and y components.

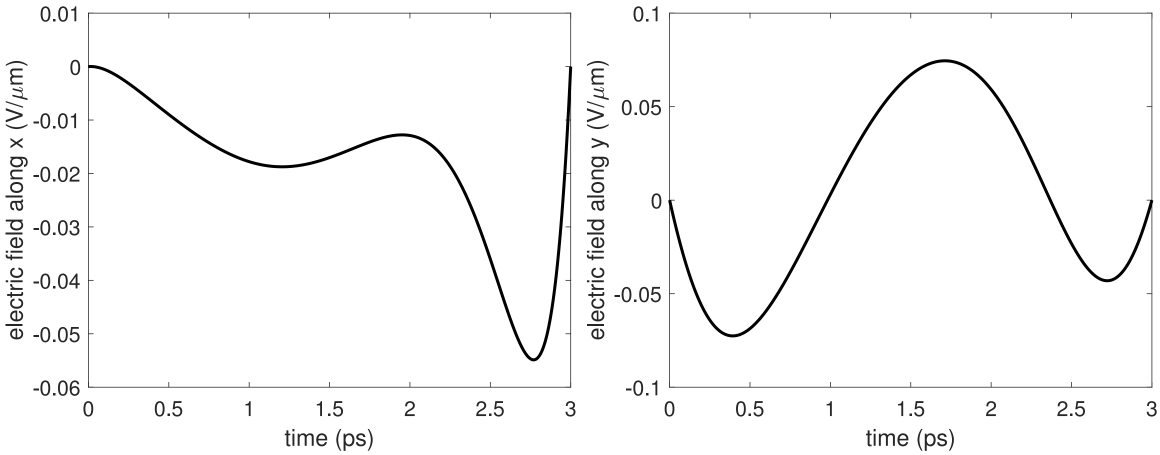

Fig. 7. Optimal electric control field versus time in the case of the desired trajectory given by (7.2); x and y components.

In the second experiment, we consider a desired trajectory $\mathbf{k}_d(t)$ given by

$$(\mathbf{k}_d(t))_x = 2\frac{t}{T}\tilde{k}, \qquad (\mathbf{k}_d(t))_y = 2\tilde{k}\sin\left(\pi\frac{(\mathbf{k}_d(t))_x}{\tilde{k}}\right), \tag{7.2}$$

For this test we adopt $T = 3$ ps, $\tilde{k} = 0.025$ nm^{-1}. In Fig. 6 the mean values of the wave-vector are shown, and in Fig. 7 the components of the optimal electric control field are depicted.

In applications, the current density is one of the physical quantities that can be measured experimentally. It is related to the mean velocity by

$$\mathbf{j} = -en\langle \mathbf{v} \rangle. \tag{7.3}$$

Given a desired profile $\mathbf{j}_d$ of the current, we can find a suitable profile $\mathbf{k}_d$ by imposing for all $t \in [0, T]$ that

$$\int_{\mathbb{R}^2} f_0(\mathbf{k} - \mathbf{k}_d(t))\mathbf{v}\, d\mathbf{k} = -\frac{\mathbf{j}_d(t)}{en}. \tag{7.4}$$

In view of this application, we consider the following desired velocity pattern

$$(\mathbf{v}_d(t))_x = (\mathbf{v}_d(t))_y = \begin{cases} 2\frac{t}{T}\alpha v_F & \text{if} \quad 0 \le t \le \frac{T}{2} \\ 2\left(1 - \frac{t}{T}\right)\alpha v_F & \text{if} \quad \frac{T}{2} \le t \le T \end{cases} \tag{7.5}$$

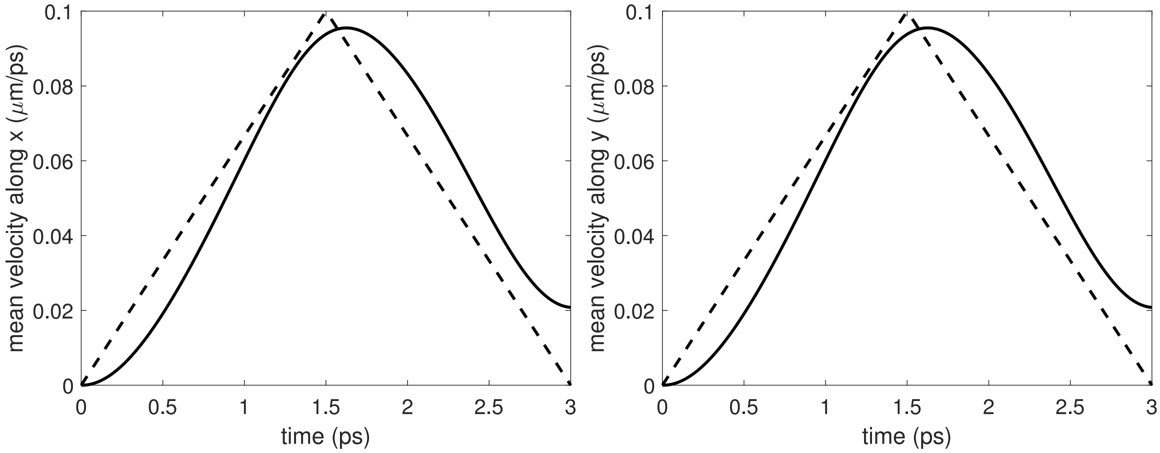

Fig. 8. Computed mean values of the velocity (continuous line) and the desired velocity (dashed line) versus time in the case of the desired trajectory given by (7.5); x (left) and y components.

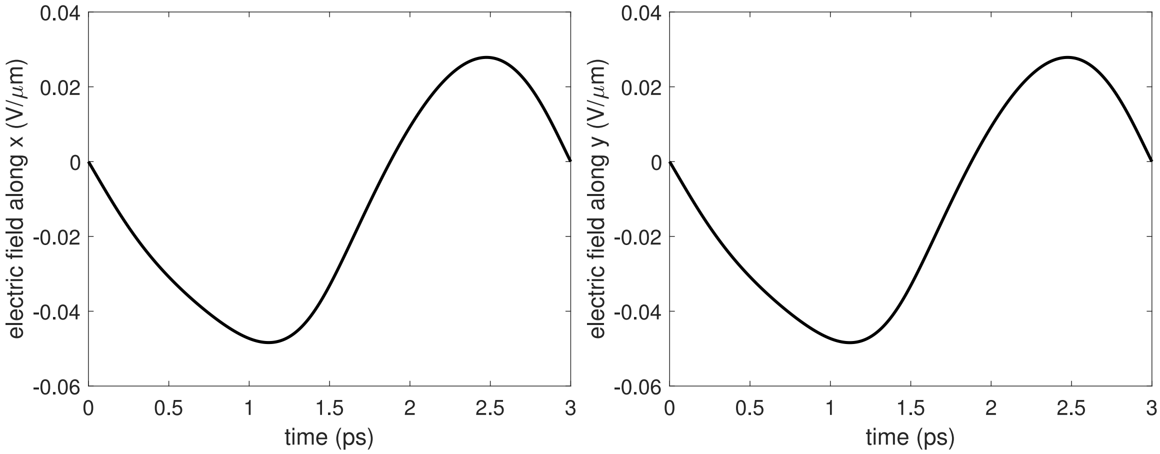

Fig. 9. Optimal electric control field versus time in the case of the desired trajectory given by (7.5); x and y components.

where $\alpha \in [0,1]$. We fix $\alpha = 0.1$.

In Fig. 8, we show the resulting mean values of velocity versus time compared with the desired one. In Fig. 9, the time behaviors of the two components of the optimal electric control field are plotted.

We conclude this section with another experiment where the purpose of the control is to steer the current density along a trajectory where the x component of the velocity linearly increases in time, while the y component has a sinusoidal behavior. We have

$$\begin{aligned} (\mathbf{v}_d(t))_x &= 2\frac{t}{T}\alpha v_F, \\ (\mathbf{v}_d(t))_y &= 2\alpha v_F \sin\left(\pi \frac{(\mathbf{v}_d(t))_x}{\alpha v_F}\right), \end{aligned} \tag{7.6}$$

where $\alpha = 0.025$.

In Fig. 10, we show the computed mean values of velocity versus time compared with the desired trajectory $\mathbf{v}_d$. In Fig. 11, the time evolution of the two components of the optimal electric control field are plotted.

8. Conclusions and acknowledgments

The formulation and analysis of ensemble optimal control problems governed by a semiclassical space-homogeneous Boltzmann equation for charge transport in graphene was presented. In this formulation, the control function was a continuous external electric field, and the purpose of this control was to drive the ensemble of charged particles to follow a given trajectory. For this purpose, an ensemble cost functional with Fermi–Dirac valley and $H^1(0,T)$ control costs was considered. Many theoretical aspects of the resulting

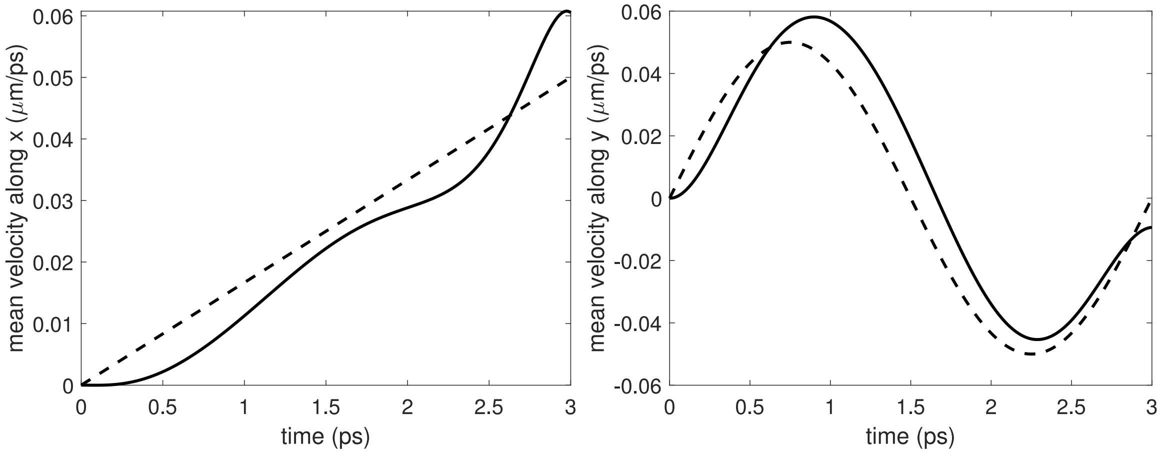

Fig. 10. Computed mean values of the velocity (continuous line) and the desired velocity (dashed line) versus time in the case of the desired trajectory given by (7.6); x (left) and y components.

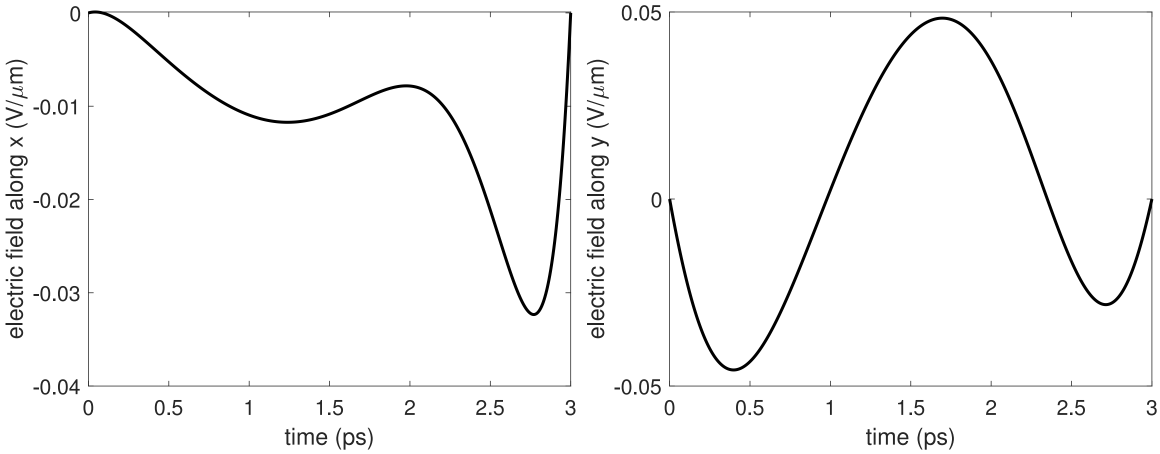

Fig. 11. Optimal electric control field versus time in the case of the desired trajectory given by (7.6); x and y components.

optimal control problem were investigated and the characterization of these controls by the corresponding optimality system was illustrated. This system was approximated by a discontinuous Galerkin scheme and solved by a nonlinear conjugate gradient method with the use of H^1 gradients. Results of numerical experiments were presented that successfully validated the effectiveness of the proposed control framework.

CRediT authorship contribution statement

Giovanni Nastasi: Conceptualization, Formal analysis, Funding acquisition, Investigation, Methodology, Supervision, Validation, Visualization, Writing – original draft, Writing – review & editing. **Alfio Borzì:** Conceptualization, Formal analysis, Investigation, Methodology, Supervision, Validation, Visualization, Writing – original draft, Writing – review & editing. **Vittorio Romano:** Conceptualization, Formal analysis, Funding acquisition, Investigation, Methodology, Supervision, Validation, Visualization, Writing – original draft, Writing – review & editing.

Declaration of competing interest

The authors declare that they have no known competing financial interests or personal relationships that could have appeared to influence the work reported in this paper.

Data availability

No data was used for the research described in the article.

Acknowledgments

The authors G.N. and V.R. acknowledge the support from INdAM, Italy (GNFM). The author V.R. acknowledges the support from MUR project PRIN 2022 "Transport phenomena in low dimensional structures: models, simulations and theoretical aspect" CUP E53D23005900006. G.N acknowledges the financial support from the project PON R&I 2014–2020 "Asse IV - Istruzione e ricerca per il recupero - REACT-EU, Azione IV.4 - Dottorati e contratti di ricerca su tematiche dell'innovazione", project "Modellizzazione, simulazione e design di transistori innovativi" and the support from Progetto di Ricerca GNFM-INDAM 2023 "Uncertainty quantification for kinetic models describing physical and socio-economical phenomena" CUP E53C2200193000.

Appendix A

In this appendix section, we prove Theorem 1.

We define the following quantities

$$A(f) = \int_{\mathbb{R}^2} S_\sigma(\mathbf{k}', \mathbf{k}) f(t, \mathbf{k}')\, d\mathbf{k}',$$
$$B(f) = \int_{\mathbb{R}^2} S_\sigma(\mathbf{k}, \mathbf{k}')(1 - f(t, \mathbf{k}'))\, d\mathbf{k}'. \tag{A.1}$$

Then the collision term C_σ writes

$$C_\sigma(f)(t, \mathbf{k}) = [A(f)(t, \mathbf{k})]\,(1 - f(t, \mathbf{k})) - [B(f)(t, \mathbf{k})]\, f(t, \mathbf{k}). \tag{A.2}$$

Therefore, if we set

$$\lambda(f) = A(f) + B(f), \tag{A.3}$$

we can write Eq. (3.1) as

$$\partial_t f + \mathbf{u}(t) \cdot \nabla_{\mathbf{k}} f + \lambda(f) f = A(f). \tag{A.4}$$

Now, we define an iterative sequence $\{f^l(t, \mathbf{k})\}$ with $f^0(t, \mathbf{k}) = f_0(\mathbf{k})$ for all $t \in [0, T]$ and given f^l we obtain f^{l+1} as solution of

$$\begin{cases} \partial_t f^{l+1} + \mathbf{u}(t) \cdot \nabla_{\mathbf{k}} f^{l+1} + \lambda(f^l) f^{l+1} = A(f^l), \\ f^{l+1}(0, \mathbf{k}) = f_0(\mathbf{k}). \end{cases} \tag{A.5}$$

Proposition 2. *The functions of the iterative sequence $\{f^l\}$ satisfy*

(i) $0 \le f^l(t, \mathbf{k}) \le 1, \quad (t, \mathbf{k}) \in [0, T] \times \mathbb{R}^2,$
(ii) *f^l is uniformly bounded in $L^\infty((0, T), L^1(\mathbb{R}^2))$ for each l.*

Proof. Since (A3) holds, $f^0 = f_0$ satisfies (i). We assume f^l satisfies (i), then f^{l+1} solving (A.5) satisfies $f^{l+1} \ge 0$ because $A(f^l) \ge 0$ and $\lambda(f^l) \ge 0$ since (A1). We notice that

$$\begin{aligned} &\partial_t(1 - f^{l+1}) + \mathbf{u}(t) \cdot \nabla_{\mathbf{k}}(1 - f^{l+1}) + \lambda(f^l)(1 - f^{l+1}) \\ &= -\partial_t f^{l+1} - \mathbf{u}(t) \cdot \nabla_{\mathbf{k}} f^{l+1} - \lambda(f^l) f^{l+1} + \lambda(f^l) \\ &= -A(f^l) + \lambda(f^l) = B(f^l). \end{aligned}$$

Moreover, for the initial condition it holds

$$1 - f^{l+1}(0, \mathbf{k}) = 1 - f_0(\mathbf{k}) \ge 0 \tag{A.6}$$

and $B(f^l) \ge 0$ since the condition (A1). Therefore, $v = 1 - f^{l+1}$ solves the equation

$$\partial_t v + \mathbf{u}(t) \cdot \nabla_{\mathbf{k}} v + \lambda(f^l) v = B(f^l), \tag{A.7}$$

with $v(0, \mathbf{k}) \ge 0$. Thus, $v(t, \mathbf{k}) \ge 0$ for all $(t, \mathbf{k}) \in [0, T] \times \mathbb{R}^2$, therefore $f^{l+1}(t, \mathbf{k}) \le 1$ for all $(t, \mathbf{k}) \in [0, T] \times \mathbb{R}^2$. Consequently, f^{l+1} satisfies (i).

In order to prove (ii), first we observe that condition (ii) holds for f_0 since (A1). Next, we suppose it holds for f^l and we integrate (A.5) in $[0, t] \times \mathbb{R}^2$ with $t \in [0, T]$. We obtain

$$\begin{aligned} &\int_{\mathbb{R}^2} f^{l+1}(t, \mathbf{k})\, d\mathbf{k} - \int_{\mathbb{R}^2} f^{l+1}(0, \mathbf{k})\, d\mathbf{k} + \int_0^t \mathbf{u}(t) \cdot \int_{\mathbb{R}^2} \nabla_{\mathbf{k}} f^{l+1}(t, \mathbf{k})\, d\mathbf{k} \\ &+ \int_0^t \int_{\mathbb{R}^2} \lambda(f^l) f^{l+1}(t, \mathbf{k})\, d\mathbf{k}\, dt = \int_0^t \int_{\mathbb{R}^2} A(f^l)\, d\mathbf{k}\, dt. \end{aligned} \tag{A.8}$$

Since

$$\int_{\mathbb{R}^2} \nabla_{\mathbf{k}} f^{l+1}(t, \mathbf{k}) = 0 \qquad \text{and} \qquad \int_0^t \int_{\mathbb{R}^2} \lambda(f^l) f^{l+1}(t, \mathbf{k})\, d\mathbf{k}\, dt \ge 0, \tag{A.9}$$

then from (A.8) it follows that

$$\left\|f^{l+1}(t,\cdot)\right\|_{L^1(\mathbb{R}^2)} \leq \|f_0\|_{L^1(\mathbb{R}^2)} + \int_0^t \left\|A(f^l)(s,\cdot)\right\|_{L^1(\mathbb{R}^2)} ds. \tag{A.10}$$

We observe that

$$\begin{aligned}\left\|A(f^l)(s,\cdot)\right\|_{L^1(\mathbb{R}^2)} &= \int_{\mathbb{R}^2}\left[\int_{\mathbb{R}^2} S_\sigma(\mathbf{k}',\mathbf{k}) f^l(t,\mathbf{k}')\,d\mathbf{k}'\right] d\mathbf{k}\\ &= \int_{\mathbb{R}^2} f^l(s,\mathbf{k}')\left[\int_{\mathbb{R}^2} S_\sigma(\mathbf{k}',\mathbf{k})\,d\mathbf{k}\right] d\mathbf{k}'\\ &\leq \left[\sup_{\mathbf{k}'\in\mathbb{R}^2}\int_{\mathbb{R}^2} S_\sigma(\mathbf{k}',\mathbf{k})\,d\mathbf{k}\right]\left\|f^l(s,\cdot)\right\|_{L^1(\mathbb{R}^2)},\end{aligned}$$

where the last step is achieved by means of (A1). Thus, by setting

$$C(S_\sigma) = \sup_{\mathbf{k}'\in\mathbb{R}^2}\int_{\mathbb{R}^2} S_\sigma(\mathbf{k}',\mathbf{k})\,d\mathbf{k}, \tag{A.11}$$

we can write (A.10) as

$$\left\|f^{l+1}(t,\cdot)\right\|_{L^1(\mathbb{R}^2)} \leq \|f_0\|_{L^1(\mathbb{R}^2)} + C(S_\sigma)\int_0^t \left\|f^l(s,\cdot)\right\|_{L^1(\mathbb{R}^2)} ds. \tag{A.12}$$

Next, we notice that $\|f_0\|_{L^1(\mathbb{R}^2)}$ is bounded by hypothesis and we observe that

$$\left\|f^1(t,\cdot)\right\|_{L^1(\mathbb{R}^2)} \leq \|f_0\|_{L^1(\mathbb{R}^2)} + t\,C(S_\sigma)\,\|f_0\|_{L^1(\mathbb{R}^2)}, \tag{A.13}$$

and furthermore

$$\begin{aligned}\left\|f^2(t,\cdot)\right\|_{L^1(\mathbb{R}^2)} &\leq \|f_0\|_{L^1(\mathbb{R}^2)} + \int_0^t C(S_\sigma)\left(\|f_0\|_{L^1(\mathbb{R}^2)} + tC(S_\sigma)\,\|f_0\|_{L^1(\mathbb{R}^2)}\right) ds\\ &= \|f_0\|_{L^1(\mathbb{R}^2)}\left(1 + C(S_\sigma)t + \left(C(S_\sigma)\right)^2\frac{t^2}{2}\right).\end{aligned}$$

Now, we proceed by induction. We suppose that

$$\left\|f^l(t,\cdot)\right\|_{L^1(\mathbb{R}^2)} \leq \|f_0\|_{L^1(\mathbb{R}^2)}\left(1 + C(S_\sigma)t + \left(C(S_\sigma)\right)^2\frac{t^2}{2} + \cdots + \left(C(S_\sigma)\right)^l\frac{t^l}{l!}\right)$$

than from (A.12) we have

$$\begin{aligned}\left\|f^{l+1}(t,\cdot)\right\|_{L^1(\mathbb{R}^2)} &\leq \|f_0\|_{L^1(\mathbb{R}^2)} + C(S_\sigma)\int_0^t\left(1 + C(S_\sigma)t + \left(C(S_\sigma)\right)^2\frac{t^2}{2} + \cdots + \left(C(S_\sigma)\right)^l\frac{t^l}{l!}\right) ds\\ &= \|f_0\|_{L^1(\mathbb{R}^2)}\left(1 + C(S_\sigma)t + \left(C(S_\sigma)\right)^2\frac{t^2}{2} + \cdots + \left(C(S_\sigma)\right)^{l+1}\frac{t^{l+1}}{(l+1)!}\right).\end{aligned}$$

Consequently, for all l we have

$$\begin{aligned}\left\|f^l(t,\cdot)\right\|_{L^1(\mathbb{R}^2)} &\leq \|f_0\|_{L^1(\mathbb{R}^2)}\left(1 + C(S_\sigma)t + \left(C(S_\sigma)\right)^2\frac{t^2}{2} + \cdots + \left(C(S_\sigma)\right)^l\frac{t^l}{l!}\right)\\ &\leq \|f_0\|_{L^1(\mathbb{R}^2)}\exp(C(S_\sigma)t)\\ &\leq \|f_0\|_{L^1(\mathbb{R}^2)}\exp(C(S_\sigma)T) =: C_1(S_\sigma,T),\end{aligned}$$

therefore (ii) is proved. □

Lemma 1. *Assume that f_0 satisfies condition (A3), and define*

$$y^l(t,\mathbf{k}) = (1+|\mathbf{k}|^2)^{\gamma/2} f^l(t,\mathbf{k}), \tag{A.14}$$

then it holds

$$\left\|y^l(t,\cdot)\right\|_{L^\infty(\mathbb{R}^2)} \leq C_2(\gamma,S_\sigma,f_0,T), \qquad t\in[0,T]. \tag{A.15}$$

Proof. Let us multiply Eq. (A.5) by $(1+|\mathbf{k}|^2)^{\gamma/2}$ getting

$$\partial_t y^{l+1} + \mathbf{u}(t)\cdot\nabla_{\mathbf{k}} y^{l+1} - \mathbf{u}(t)\cdot\left(\nabla_{\mathbf{k}}\left(1+|\mathbf{k}|^2\right)^{\gamma/2}\right) f^{l+1} + \lambda(f^l)y^{l+1} = \left(1+|\mathbf{k}|^2\right)^{\gamma/2} A(f^l). \tag{A.16}$$

We remark that

$$\nabla_{\mathbf{k}}\left(1+|\mathbf{k}|^2\right)^{\gamma/2} = \gamma\left(1+|\mathbf{k}|^2\right)^{\frac{\gamma-2}{2}}\mathbf{k} \tag{A.17}$$

and therefore we obtain

$$\partial_t y^{l+1} + \mathbf{u}(t) \cdot \nabla_{\mathbf{k}} y^{l+1} + \lambda(f^l) y^{l+1} = R_1^{l+1} + R_2^l, \tag{A.18}$$

where

$$R_1^{l+1}(t,\mathbf{k}) = \gamma \left(\mathbf{u}(t)\cdot\mathbf{k}\right)\left(1+|\mathbf{k}|^2\right)^{\frac{\gamma-2}{2}} f^{l+1}(t,\mathbf{k}), \tag{A.19}$$

$$R_2^l(t,\mathbf{k}) = \left(1+|\mathbf{k}|^2\right)^{\gamma/2} A(f^l)(t,\mathbf{k}). \tag{A.20}$$

Thus, for all $t \in [0,T]$, we have

$$\begin{aligned}\left\|R_1^{l+1}(t,\mathbf{k})\right\|_{L^\infty(\mathbb{R}^2)} &\le \gamma \max_{t\in[0,T]} |\mathbf{u}(t)| \left\|\left(1+|\mathbf{k}|^2\right)^{1/2}\left(1+|\mathbf{k}|^2\right)^{\frac{\gamma-2}{2}} f^{l+1}(t,\mathbf{k})\right\|_{L^\infty(\mathbb{R}^2)} \\ &= \gamma \left\|\mathbf{u}(t)\right\|_\infty \left\|\left(1+|\mathbf{k}|^2\right)^{\frac{\gamma-1}{2}} f^{l+1}(t,\mathbf{k})\right\|_{L^\infty(\mathbb{R}^2)}\end{aligned}$$

Now, for all $g \in L^\infty(\mathbb{R}^2)$, the following inequality holds [34]

$$\left\|\left(1+|\mathbf{k}|^2\right)^{\frac{\gamma-1}{2}} g(\mathbf{k})\right\|_{L^\infty(\mathbb{R}^2)} \le C(\gamma) \left\|g(\mathbf{k})\right\|_{L^\infty(\mathbb{R}^2)}^{\frac{1}{\gamma}} \left\|\left(1+|\mathbf{k}|^2\right)^{\frac{\gamma}{2}} g(\mathbf{k})\right\|_{L^\infty(\mathbb{R}^2)}^{1-\frac{1}{\gamma}}. \tag{A.21}$$

Thus, for $g = f^{l+1}$ and for all $t \in [0,T]$

$$\begin{aligned}\left\|\left(1+|\mathbf{k}|^2\right)^{\frac{\gamma-1}{2}} f^{l+1}(t,\mathbf{k})\right\|_{L^\infty(\mathbb{R}^2)} &\le C(\gamma) \left\|f^{l+1}(t,\mathbf{k})\right\|_{L^\infty(\mathbb{R}^2)}^{\frac{1}{\gamma}} \left\|\left(1+|\mathbf{k}|^2\right)^{\frac{\gamma}{2}} f^{l+1}(t,\mathbf{k})\right\|_{L^\infty(\mathbb{R}^2)}^{1-\frac{1}{\gamma}} \\ &\le C(\gamma) \left\|\left(1+|\mathbf{k}|^2\right)^{\frac{\gamma}{2}} f^{l+1}(t,\mathbf{k})\right\|_{L^\infty(\mathbb{R}^2)}^{\frac{1}{\gamma}} \left\|\left(1+|\mathbf{k}|^2\right)^{\frac{\gamma}{2}} f^{l+1}(t,\mathbf{k})\right\|_{L^\infty(\mathbb{R}^2)}^{1-\frac{1}{\gamma}} \\ &= C(\gamma) \left\|y^{l+1}(t,\mathbf{k})\right\|_{L^\infty(\mathbb{R}^2)}.\end{aligned}$$

Moreover, for all $t \in [0,T]$, we get

$$\begin{aligned}\left\|R_2^l(t,\mathbf{k})\right\|_{L^\infty(\mathbb{R}^2)} &= \left\|\left(1+|\mathbf{k}|^2\right)^{\gamma/2} \int_{\mathbb{R}^2} S_\sigma(\mathbf{k}',\mathbf{k}) f^l(t,\mathbf{k}')\, d\mathbf{k}'\right\|_{L^\infty(\mathbb{R}^2)} \\ &\le \left\|\left(1+|\mathbf{k}|^2\right)^{\gamma/2} \int_{\mathbb{R}^2} S_\sigma(\mathbf{k}',\mathbf{k}) \left(1+|\mathbf{k}'|^2\right)^{\gamma/2} f^l(t,\mathbf{k}')\, d\mathbf{k}'\right\|_{L^\infty(\mathbb{R}^2)} \\ &\le \left\|y^l(t,\mathbf{k})\right\|_{L^\infty(\mathbb{R}^2)} \left\|\left(1+|\mathbf{k}|^2\right)^{\gamma/2} \int_{\mathbb{R}^2} S_\sigma(\mathbf{k}',\mathbf{k})\, d\mathbf{k}'\right\|_{L^\infty(\mathbb{R}^2)} \\ &\le \left\|y^l(t,\mathbf{k})\right\|_{L^\infty(\mathbb{R}^2)} C(S_\sigma,\gamma),\end{aligned}$$

where the last step is achieved by condition (A2). Thus, we have

$$\left\|R_1^{l+1}(t,\mathbf{k})\right\|_{L^\infty(\mathbb{R}^2)} \le \tilde{C}_1 \left\|y^{l+1}(t,\mathbf{k})\right\|_{L^\infty(\mathbb{R}^2)}, \tag{A.22}$$

$$\left\|R_2^l(t,\mathbf{k})\right\|_{L^\infty(\mathbb{R}^2)} \le \tilde{C}_2 \left\|y^l(t,\mathbf{k})\right\|_{L^\infty(\mathbb{R}^2)}, \tag{A.23}$$

where we have set $\tilde{C}_1 = \gamma C(\gamma) \left\|\mathbf{u}(t)\right\|_\infty$ and $\tilde{C}_2 = C(S_\sigma,\gamma)$.

Let us consider Eq. (A.18). Recalling that $\lambda(f^l) \ge 0$, for all $t \in [0,T]$ by time integration along characteristics (see, e.g., [35]) and taking the supremum we obtain

$$\left\|y^{l+1}(t,\mathbf{k})\right\|_{L^\infty(\mathbb{R}^2)} \le \left\|y^{l+1}(0,\mathbf{k})\right\|_{L^\infty(\mathbb{R}^2)} + \int_0^t \left(\left\|R_1^{l+1}(s,\mathbf{k})\right\|_{L^\infty(\mathbb{R}^2)} + \left\|R_2^l(s,\mathbf{k})\right\|_{L^\infty(\mathbb{R}^2)}\right) ds \tag{A.24}$$

Now, by means of (A.22) and (A.23) we get

$$\left\|y^{l+1}(t,\mathbf{k})\right\|_{L^\infty(\mathbb{R}^2)} \le \left\|y^{l+1}(0,\mathbf{k})\right\|_{L^\infty(\mathbb{R}^2)} + \int_0^t \left(\tilde{C}_1 \left\|y^{l+1}(s,\mathbf{k})\right\|_{L^\infty(\mathbb{R}^2)} + \tilde{C}_2 \left\|y^l(s,\mathbf{k})\right\|_{L^\infty(\mathbb{R}^2)}\right) ds. \tag{A.25}$$

Since (A3) holds, we have that

$$\left\|y^{l+1}(0,\mathbf{k})\right\|_{L^\infty(\mathbb{R}^2)} = \left\|\left(1+|\mathbf{k}|^2\right)^{\gamma/2} f_0(\mathbf{k})\right\|_{L^\infty(\mathbb{R}^2)} =: \tilde{C}_0. \tag{A.26}$$

Thus, we obtain

$$\left\|y^{l+1}(t,\mathbf{k})\right\|_{L^\infty(\mathbb{R}^2)} \le \tilde{C}_0 + \tilde{C}_1 \int_0^t \left\|y^{l+1}(s,\mathbf{k})\right\|_{L^\infty(\mathbb{R}^2)} ds + \tilde{C}_2 \int_0^t \left\|y^l(s,\mathbf{k})\right\|_{L^\infty(\mathbb{R}^2)} ds. \tag{A.27}$$

Following [34], we define

$$\alpha_l(t) = \left\|y^l(t,\mathbf{k})\right\|_{L^\infty(\mathbb{R}^2)}, \tag{A.28}$$

then we obtain

$$\alpha_{l+1}(t) \le \tilde{C}_0 + \tilde{C}_1 \int_0^t \alpha_{l+1}(s)\, ds + \tilde{C}_2 \int_0^t \alpha_l(s)\, ds. \tag{A.29}$$

Let $\beta = \beta(t)$ solution of the Cauchy problem

$$\begin{cases} \beta'(t) = (\tilde{C}_1 + \tilde{C}_2)\beta(t) \\ \beta(0) = \tilde{C}_0 \end{cases} \tag{A.30}$$

and we prove by induction that

$$\alpha_l(t) \le \beta(t), \qquad t \ge 0, \quad l \in \mathbb{N}. \tag{A.31}$$

Clearly, we have

$$\alpha_0(t) = \tilde{C}_0 = \beta(0) \le \beta(t), \qquad t \ge 0. \tag{A.32}$$

We define

$$\psi_{l+1}(t) = \tilde{C}_0 + \tilde{C}_1 \int_0^t \alpha_{l+1}(s)\, ds + \tilde{C}_2 \int_0^t \alpha_l(s)\, ds \tag{A.33}$$

hence, we have $\alpha_{l+1}(t) \le \psi_{l+1}(t)$ for all $t \ge 0$. Now, we consider the set

$$\tau = \left\{ t \ge 0 \,:\, \psi_{l+1}(s) \le \beta(s), \quad s \in [0,t) \right\}. \tag{A.34}$$

We show that τ is unbounded. For this aim, we suppose by contradiction that there exists $\bar{t} \ge 0$ such that

$$\psi_{l+1}(\bar{t}) = \beta(\bar{t}), \qquad \text{and} \qquad \psi'_{l+1}(\bar{t}) > \beta'(\bar{t}). \tag{A.35}$$

Thus, we have

$$\begin{aligned} \psi'_{l+1}(\bar{t}) &= \tilde{C}_1 \alpha_{l+1}(\bar{t}) + \tilde{C}_2 \alpha_l(\bar{t}) \le \tilde{C}_1 \psi_{l+1}(\bar{t}) + \tilde{C}_2 \beta(\bar{t}) \\ &= (\tilde{C}_1 + \tilde{C}_2)\beta(\bar{t}) = \beta'(\bar{t}), \end{aligned}$$

that is a contradiction. Consequently, we have that $\alpha_{l+1}(t) \le \psi_{l+1}(t) \le \beta(t)$ for all $t \ge 0$ and then Eq. (A.31) holds. Therefore, for all $l \in \mathbb{N}$, we have that

$$\left\| y^l(t,\mathbf{k}) \right\|_{L^\infty(\mathbb{R}^2)} \le \beta(t) = \tilde{C}_0 \exp[(\tilde{C}_1 + \tilde{C}_2)t] \le \tilde{C}_0 \exp[(\tilde{C}_1 + \tilde{C}_2)T] =: C_2, \qquad t \in [0,T], \tag{A.36}$$

by noticing that $C_2 = C_2(\gamma, S_\sigma, f_0, T)$, the proof is concluded. □

Next, we analyze the convergence properties of the sequence $\left\{ \nabla_{\mathbf{k}} f^l \right\}$.

Lemma 2. *The sequence* $\left\{ \nabla_{\mathbf{k}} f^l \right\}$ *is uniformly bounded in* $L^\infty\left([0,T], L^1(\mathbb{R}^2) \cap L^\infty(\mathbb{R}^2)\right)$.

Proof. First, we formally differentiate Eq. (A.5) with respect to $\mathbf{k}$ obtaining

$$\partial_t \left(\nabla_{\mathbf{k}} f^{l+1}\right) + \mathbf{u}(t)\nabla_{\mathbf{k}} \left(\nabla_{\mathbf{k}} f^{l+1}\right) + \lambda(f^l)\nabla_{\mathbf{k}} f^{l+1} = -\left(\nabla_{\mathbf{k}} \lambda(f^l)\right) f^{l+1} + \nabla_{\mathbf{k}} A(f^l), \tag{A.37}$$

where $\nabla_{\mathbf{k}} \left(\nabla_{\mathbf{k}} f^{l+1}\right)$ denotes the Hessian matrix of f^{l+1}. Further, we multiply the last equation by $\left(1 + |\mathbf{k}|^2\right)^{\gamma/2}$ and we define

$$\mathbf{z}^l(t,\mathbf{k}) = \left(1 + |\mathbf{k}|^2\right)^{\gamma/2} \nabla_{\mathbf{k}} f^l(t,\mathbf{k}), \tag{A.38}$$

obtaining

$$\begin{aligned} &\partial_t \mathbf{z}^{l+1} + \mathbf{u}(t)\nabla_{\mathbf{k}} \mathbf{z}^{l+1} + \lambda(f^l)\mathbf{z}^{l+1} \\ &= \mathbf{u}(t)\left[\nabla_{\mathbf{k}} \left(1 + |\mathbf{k}|^2\right)^{\gamma/2} \cdot \left(\nabla_{\mathbf{k}} f^{l+1}\right)\right] - \left(1 + |\mathbf{k}|^2\right)^{\gamma/2} \left[\nabla_{\mathbf{k}} \lambda(f^l)\right] f^{l+1} + \left(1 + |\mathbf{k}|^2\right)^{\gamma/2} \nabla_{\mathbf{k}} A(f^l) \end{aligned} \tag{A.39}$$

Recalling that $\lambda(f^l) = A(f^l) + B(f^l)$, we obtain

$$\partial_t \mathbf{z}^{l+1} + \mathbf{u}(t)\nabla_{\mathbf{k}} \mathbf{z}^{l+1} + \lambda(f^l)\mathbf{z}^{l+1} = P_1 + P_2 + P_3, \tag{A.40}$$

where

$$\begin{aligned} P_1 &= \left(1 + |\mathbf{k}|^2\right)^{\gamma/2} \nabla_{\mathbf{k}} A(f^l)(1 - f^{l+1}) \\ P_2 &= -\left(1 + |\mathbf{k}|^2\right)^{\gamma/2} \nabla_{\mathbf{k}} B(f^l) f^{l+1} \\ P_3 &= \gamma \left(1 + |\mathbf{k}|^2\right)^{\frac{\gamma-2}{2}} \{\mathbf{u}(t), \mathbf{k}\} \cdot \nabla_{\mathbf{k}} f^{l+1}, \end{aligned}$$

where the symbol $\{\cdot,\cdot\}$ indicates the Hadamard product.

Now, we proceed as in Lemma 1 and we obtain

$$\left\|z^{l+1}(t,\mathbf{k})\right\|_{L^\infty(\mathbb{R}^2)} \le \left\|z^{l+1}(0,\mathbf{k})\right\|_{L^\infty(\mathbb{R}^2)} + \int_0^t \left(\left\|P_1(s,\mathbf{k})\right\|_{L^\infty(\mathbb{R}^2)} + \left\|P_2(s,\mathbf{k})\right\|_{L^\infty(\mathbb{R}^2)} + \left\|P_3(s,\mathbf{k})\right\|_{L^\infty(\mathbb{R}^2)}\right) ds. \tag{A.41}$$

Next, we estimate $\|P_1(t,\mathbf{k})\|_{L^\infty(\mathbb{R}^2)}$, $\|P_2(t,\mathbf{k})\|_{L^\infty(\mathbb{R}^2)}$ and $\|P_3(t,\mathbf{k})\|_{L^\infty(\mathbb{R}^2)}$. To estimate $\|P_1(t,\mathbf{k})\|_{L^\infty(\mathbb{R}^2)}$, by Proposition 2, we get

$$\begin{aligned}
\|P_1(t,\mathbf{k})\|_{L^\infty(\mathbb{R}^2)} &\le \left\|\left(1+|\mathbf{k}|^2\right)^{\gamma/2} \nabla_{\mathbf{k}} A(f^l)\right\|_{L^\infty(\mathbb{R}^2)} \\
&= \left\|\left(1+|\mathbf{k}|^2\right)^{\gamma/2} \int_{\mathbb{R}^2} \nabla_{\mathbf{k}} \left(S_\sigma(\mathbf{k}',\mathbf{k})\right) f^l(t,\mathbf{k}')\, d\mathbf{k}'\right\|_{L^\infty(\mathbb{R}^2)} \\
&\le \left\|\left(1+|\mathbf{k}|^2\right)^{\gamma/2} \int_{\mathbb{R}^2} \nabla_{\mathbf{k}} \left(S_\sigma(\mathbf{k}',\mathbf{k})\right) \left(1+|\mathbf{k}'|^2\right)^{\gamma/2} f^l(t,\mathbf{k}')\, d\mathbf{k}'\right\|_{L^\infty(\mathbb{R}^2)} \\
&\le \left\|y^l(t,\mathbf{k})\right\|_{L^\infty(\mathbb{R}^2)} \left\|\left(1+|\mathbf{k}|^2\right)^{\gamma/2} \int_{\mathbb{R}^2} \nabla_{\mathbf{k}} S_\sigma(\mathbf{k}',\mathbf{k})\, d\mathbf{k}'\right\|_{L^\infty(\mathbb{R}^2)} \\
&\le C_2(\gamma, S_\sigma, f_0, T)\, \tilde{C}(\gamma, S_\sigma),
\end{aligned}$$

where we have used Lemma 1 and the last step is achieved since $|\nabla_{\mathbf{k}} S_\sigma| \in \chi$.

For the estimate of $\|P_2(t,\mathbf{k})\|_{L^\infty(\mathbb{R}^2)}$, we have

$$\begin{aligned}
\|P_2(t,\mathbf{k})\|_{L^\infty(\mathbb{R}^2)} &\le \left\|\left(1+|\mathbf{k}|^2\right)^{\gamma/2} \nabla_{\mathbf{k}} B(f^l)\right\|_{L^\infty(\mathbb{R}^2)} \\
&= \left\|\left(1+|\mathbf{k}|^2\right)^{\gamma/2} \int_{\mathbb{R}^2} \nabla_{\mathbf{k}} \left(S_\sigma(\mathbf{k}',\mathbf{k})\right) (1-f^l(t,\mathbf{k}'))\, d\mathbf{k}'\right\|_{L^\infty(\mathbb{R}^2)} \\
&\le \left\|\left(1+|\mathbf{k}|^2\right)^{\gamma/2} \int_{\mathbb{R}^2} \nabla_{\mathbf{k}} S_\sigma(\mathbf{k}',\mathbf{k})\, d\mathbf{k}'\right\|_{L^\infty(\mathbb{R}^2)} \\
&+ \left\|\left(1+|\mathbf{k}|^2\right)^{\gamma/2} \int_{\mathbb{R}^2} \nabla_{\mathbf{k}} \left(S_\sigma(\mathbf{k}',\mathbf{k})\right) \left(1+|\mathbf{k}'|^2\right)^{\gamma/2} f^l(t,\mathbf{k}')\, d\mathbf{k}'\right\|_{L^\infty(\mathbb{R}^2)} \\
&\le \left\|\left(1+|\mathbf{k}|^2\right)^{\gamma/2} \int_{\mathbb{R}^2} \nabla_{\mathbf{k}} S_\sigma(\mathbf{k}',\mathbf{k})\, d\mathbf{k}'\right\|_{L^\infty(\mathbb{R}^2)} \\
&+ \left\|y^l(t,\mathbf{k})\right\|_{L^\infty(\mathbb{R}^2)} \left\|\left(1+|\mathbf{k}|^2\right)^{\gamma/2} \int_{\mathbb{R}^2} \nabla_{\mathbf{k}} S_\sigma(\mathbf{k}',\mathbf{k})\, d\mathbf{k}'\right\|_{L^\infty(\mathbb{R}^2)} \\
&\le (1 + C_2(\gamma, S_\sigma, f_0, T))\, \tilde{C}(\gamma, S_\sigma).
\end{aligned}$$

For the estimate of $\|P_3(t,\mathbf{k})\|_{L^\infty(\mathbb{R}^2)}$, since $|\mathbf{k}| \le (1+|\mathbf{k}|^2)^{1/2}$ for all $\mathbf{k} \in \mathbb{R}^2$ and following the same steps as in Lemma 1, we have

$$\|P_3(t,\mathbf{k})\|_{L^\infty(\mathbb{R}^2)} \le \gamma \tilde{\tilde{C}}(\gamma)\, \|\mathbf{u}(t)\|_\infty \left\|\mathbf{z}^{l+1}(t,\mathbf{k})\right\|_{L^\infty(\mathbb{R}^2)}$$

Now, we use these estimates in Eq. (A.41) obtaining

$$\left\|z^{l+1}(t,\mathbf{k})\right\|_{L^\infty(\mathbb{R}^2)} \le \left\|z^{l+1}(0,\mathbf{k})\right\|_{L^\infty(\mathbb{R}^2)} + \int_0^t \left[(1+2C_2(\gamma,S_\sigma,f_0,T))\tilde{C}(\gamma,S_\sigma) + \gamma\tilde{\tilde{C}}(\gamma)\, \|\mathbf{u}(s)\|_\infty \left\|\mathbf{z}^{l+1}(s,\mathbf{k})\right\|_{L^\infty(\mathbb{R}^2)}\right] ds$$

Since (A3) holds, we have that

$$\left\|\mathbf{z}^{l+1}(0,\mathbf{k})\right\|_{L^\infty(\mathbb{R}^2)} = \left\|\left(1+|\mathbf{k}|^2\right)^{\gamma/2} \nabla_{\mathbf{k}} f_0(\mathbf{k})\right\|_{L^\infty(\mathbb{R}^2)} =: \tilde{C}_0. \tag{A.42}$$

Furthermore, by defining

$$\begin{aligned}
\tilde{C}_1 &:= (1+2C_2(\gamma,S_\sigma,f_0,T))\tilde{C}(\gamma,S_\sigma), \\
\tilde{C}_2 &:= \gamma\tilde{\tilde{C}}(\gamma)\, \|\mathbf{u}(s)\|_\infty
\end{aligned}$$

we obtain

$$\left\|z^{l+1}(t,\mathbf{k})\right\|_{L^\infty(\mathbb{R}^2)} \le \tilde{C}_0 + t\tilde{C}_1 + \tilde{C}_2 \int_0^t \left\|z^{l+1}(s,\mathbf{k})\right\|_{L^\infty(\mathbb{R}^2)} ds.$$

Next, as in Lemma 1 we define

$$\tilde{\alpha}_l(t) = \left\|\mathbf{z}^l(t,\mathbf{k})\right\|_{L^\infty(\mathbb{R}^2)}, \tag{A.43}$$

then we obtain

$$\tilde{\alpha}_{l+1}(t) \le \tilde{C}_0 + t\tilde{C}_1 + \tilde{C}_2 \int_0^t \tilde{\alpha}_{l+1}(s)\, ds. \tag{A.44}$$

Let $\tilde{\beta} = \tilde{\beta}(t)$ be the solution of the Cauchy problem

$$\begin{cases} \tilde{\beta}'(t) = \tilde{C}_1 + \tilde{C}_2\tilde{\beta}(t) \\ \tilde{\beta}(0) = \tilde{C}_0 \end{cases} \tag{A.45}$$

We prove by induction that

$$\tilde{\alpha}_l(t) \le \tilde{\beta}(t), \qquad t \ge 0, \quad l \in \mathbb{N}. \tag{A.46}$$

Clearly, we have

$$\tilde{\alpha}_0(t) = \tilde{C}_0 = \tilde{\beta}(0) \le \tilde{\beta}(t), \qquad t \ge 0. \tag{A.47}$$

We define

$$\tilde{\psi}_{l+1}(t) = \tilde{C}_0 + t\tilde{C}_1 + \tilde{C}_2 \int_0^t \tilde{\alpha}_{l+1}(s)\, ds. \tag{A.48}$$

We have $\tilde{\alpha}_{l+1}(t) \le \tilde{\psi}_{l+1}(t)$ for all $t \ge 0$. Now, we consider the set

$$\tau = \left\{ t \ge 0 \ : \ \tilde{\psi}_{l+1}(s) \le \tilde{\beta}(s), \quad s \in [0,t) \right\}. \tag{A.49}$$

Next, we show that τ is unbounded. For this purpose, we suppose by contradiction that there exists $\bar{t} \ge 0$ such that

$$\tilde{\psi}_{l+1}(\bar{t}) = \tilde{\beta}(\bar{t}), \qquad \text{and} \qquad \tilde{\psi}'_{l+1}(\bar{t}) > \tilde{\beta}'(\bar{t}). \tag{A.50}$$

Thus, we have

$$\begin{aligned} \tilde{\psi}'_{l+1}(\bar{t}) &= \tilde{C}_1 + \tilde{C}_2\tilde{\alpha}_{l+1}(\bar{t}) \\ &\le \tilde{C}_1 + \tilde{C}_2\tilde{\psi}_{l+1}(\bar{t}) \\ &= \tilde{C}_1 + \tilde{C}_2\tilde{\beta}(\bar{t}) = \tilde{\beta}'(\bar{t}), \end{aligned}$$

which is a contradiction. Consequently, we have that $\tilde{\alpha}_{l+1}(t) \le \tilde{\psi}_{l+1}(t) \le \tilde{\beta}(t)$ for all $t \ge 0$ and then Eq. (A.46) holds. Therefore, for all $l \in \mathbb{N}$ we have that

$$\begin{aligned} \left\| \mathbf{z}^l(t,\mathbf{k}) \right\|_{L^\infty(\mathbb{R}^2)} \le \tilde{\beta}(t) &= \left(\tilde{C}_0 + \frac{\tilde{C}_1}{\tilde{C}_2} \right) \exp(\tilde{C}_2 t) - \frac{\tilde{C}_1}{\tilde{C}_2} \\ &\le \left(\tilde{C}_0 + \frac{\tilde{C}_1}{\tilde{C}_2} \right) \exp(\tilde{C}_2 T) - \frac{\tilde{C}_1}{\tilde{C}_2}, \qquad t \in [0,T]. \end{aligned}$$

To conclude the proof, we integrate in time Eq. (A.37) and we take the L^1 norms. Since $\lambda(f^l) \ge 0$ we obtain

$$\begin{aligned} \left\| \nabla_{\mathbf{k}} f^{l+1}(t,\mathbf{k}) \right\|_{L^1(\mathbb{R}^2)} &\le \left\| \nabla_{\mathbf{k}} f_0(\mathbf{k}) \right\|_{L^1(\mathbb{R}^2)} \\ &+ \int_0^t \left[\left\| \nabla_{\mathbf{k}} A(f^l(s,\mathbf{k})) \right\|_{L^1(\mathbb{R}^2)} + \left\| f^{l+1}(s,\mathbf{k}) \nabla_{\mathbf{k}} \lambda(f^l(s,\mathbf{k})) \right\|_{L^1(\mathbb{R}^2)} \right] ds. \end{aligned}$$

Now, we proceed estimating the following term

$$\left\| \nabla_{\mathbf{k}} A(f^l(t,\mathbf{k})) \right\|_{L^1(\mathbb{R}^2)} \le \int_{\mathbb{R}^2} \left[\int_{\mathbb{R}^2} \left| \nabla_{\mathbf{k}}(S_\sigma(\mathbf{k}',\mathbf{k})) \right| f^l(t,\mathbf{k}')\, d\mathbf{k}' \right] d\mathbf{k}$$

that is bounded because $\nabla_{\mathbf{k}} S_\sigma(\mathbf{k}',\mathbf{k}) \in \chi$. Moreover, we estimate the following term

$$\begin{aligned} &\left\| f^{l+1}(t,\mathbf{k}) \nabla_{\mathbf{k}} \lambda(f^l(t,\mathbf{k})) \right\|_{L^1(\mathbb{R}^2)} = \int_{\mathbb{R}^2} \left| f^{l+1}(t,\mathbf{k}) \nabla_{\mathbf{k}} \lambda(f^l(t,\mathbf{k})) \right| d\mathbf{k} \\ &\le \int_{\mathbb{R}^2} f^{l+1}(t,\mathbf{k}) \left| \left(1+|\mathbf{k}|^2\right)^{\gamma/2} \nabla_{\mathbf{k}} \lambda(f^l(t,\mathbf{k})) \right| d\mathbf{k} \\ &\le \int_{\mathbb{R}^2} f^{l+1}(t,\mathbf{k}) \left\{ \left\| \left(1+|\mathbf{k}|^2\right)^{\gamma/2} \nabla_{\mathbf{k}} A(f^l(t,\mathbf{k})) \right\|_{L^\infty(\mathbb{R}^2)} + \left\| \left(1+|\mathbf{k}|^2\right)^{\gamma/2} \nabla_{\mathbf{k}} B(f^l(t,\mathbf{k})) \right\|_{L^\infty(\mathbb{R}^2)} \right\} d\mathbf{k} \\ &\le \left\| f^{l+1}(t,\mathbf{k}) \right\|_{L^1(\mathbb{R}^2)} \left\{ \left\| \left(1+|\mathbf{k}|^2\right)^{\gamma/2} \nabla_{\mathbf{k}} A(f^l(t,\mathbf{k})) \right\|_{L^\infty(\mathbb{R}^2)} + \left\| \left(1+|\mathbf{k}|^2\right)^{\gamma/2} \nabla_{\mathbf{k}} B(f^l(t,\mathbf{k})) \right\|_{L^\infty(\mathbb{R}^2)} \right\}. \end{aligned}$$

Now, we can use the estimates for P_1 and P_2 to estimate $\left\| \left(1+|\mathbf{k}|^2\right)^{\gamma/2} \nabla_{\mathbf{k}} A(f^l(t,\mathbf{k})) \right\|_{L^\infty(\mathbb{R}^2)}$ and $\left\| \left(1+|\mathbf{k}|^2\right)^{\gamma/2} \nabla_{\mathbf{k}} B(f^l(t,\mathbf{k})) \right\|_{L^\infty(\mathbb{R}^2)}$ respectively and, further, we can use Proposition 2 (ii) to estimate $\left\| f^{l+1}(t,\mathbf{k}) \right\|_{L^1(\mathbb{R}^2)}$. We obtain a constant depending on f_0, γ, S_σ, T such that

$$\left\| \nabla_{\mathbf{k}} f^l(t,\mathbf{k}) \right\|_{L^1(\mathbb{R}^2)} \le C_3(\gamma, S_\sigma, f_0, T), \tag{A.51}$$

that concludes the proof. □

With Proposition 2, Lemmas 1 and 2 we have weak-∗ convergence of sequences

(1) $f^l \rightharpoonup f$ in $L^\infty([0,T], L^\infty(\mathbb{R}^2))$;
(2) $(1+|\mathbf{k}|^2)^{\gamma/2} f^l \rightharpoonup (1+|\mathbf{k}|^2)^{\gamma/2} f$ in $L^\infty([0,T], L^\infty(\mathbb{R}^2))$;
(3) $(1+|\mathbf{k}|^2)^{\gamma/2} \nabla_{\mathbf{k}} f^l \rightharpoonup (1+|\mathbf{k}|^2)^{\gamma/2} \nabla_{\mathbf{k}} f$ in $L^\infty([0,T], L^\infty(\mathbb{R}^2))$.

Indeed

(1) It follows from Proposition 2.
(2) Since $f^l \rightharpoonup f$ in the weak-$*$ topology, for all $u \in L^1(\mathbb{R}^2)$ we have
$$\int_{\mathbb{R}^2} u(\mathbf{k}) f^l(\mathbf{k})\, d\mathbf{k} \longrightarrow \int_{\mathbb{R}^2} u(\mathbf{k}) f(\mathbf{k})\, d\mathbf{k}.$$
If $u \in L^1(\mathbb{R}^2)$ then
$$\frac{u(\mathbf{k})}{(1+\mathbf{k}^2)^{\gamma/2}} \in L^1(\mathbb{R}^2).$$
We have
$$\int_{\mathbb{R}^2} u(\mathbf{k}) f^l(\mathbf{k})\, d\mathbf{k} = \int_{\mathbb{R}^2} \frac{u(\mathbf{k})}{(1+\mathbf{k}^2)^{\gamma/2}} (1+\mathbf{k}^2)^{\gamma/2} f^l(\mathbf{k})\, d\mathbf{k} \tag{A.52}$$
and also
$$\int_{\mathbb{R}^2} u(\mathbf{k}) f(\mathbf{k})\, d\mathbf{k} = \int_{\mathbb{R}^2} \frac{u(\mathbf{k})}{(1+\mathbf{k}^2)^{\gamma/2}} (1+\mathbf{k}^2)^{\gamma/2} f(\mathbf{k})\, d\mathbf{k}. \tag{A.53}$$
Since $(1+\mathbf{k}^2)^{\gamma/2} f^l(\mathbf{k})$ is uniformly bounded in $L^\infty(\mathbb{R}^2)$, one has
$$\int_{\mathbb{R}^2} \frac{u(\mathbf{k})}{(1+\mathbf{k}^2)^{\gamma/2}} (1+\mathbf{k}^2)^{\gamma/2} f^l(\mathbf{k})\, d\mathbf{k} \longrightarrow \int_{\mathbb{R}^2} \frac{u(\mathbf{k})}{(1+\mathbf{k}^2)^{\gamma/2}} (1+\mathbf{k}^2)^{\gamma/2} f(\mathbf{k})\, d\mathbf{k}.$$
For the uniqueness of the weak limit, by choosing as test function $u(\mathbf{k})/(1+\mathbf{k}^2)^{\gamma/2}$ we get that $(1+\mathbf{k}^2)^{\gamma/2} f^l(\mathbf{k}) \rightharpoonup (1+\mathbf{k}^2)^{\gamma/2} f(\mathbf{k})$ in the weak-$*$ topology.
(3) Let $\mathbf{u} \in (L^1(\mathbb{R}^2))^2$ such that
$$\nabla_{\mathbf{k}} \cdot \mathbf{u} \in L^1(\mathbb{R}^2), \qquad \lim_{|\mathbf{k}|\to\infty} \mathbf{u}(\mathbf{k}) = \mathbf{0}, \qquad \lim_{|\mathbf{k}|\to\infty} \nabla_{\mathbf{k}} \cdot \mathbf{u}(\mathbf{k}) = 0.$$
One has
$$\begin{aligned}\int_{\mathbb{R}^2} \mathbf{u}(\mathbf{k}) \cdot \nabla_{\mathbf{k}} f^l(\mathbf{k})\, d\mathbf{k} &= -\int_{\mathbb{R}^2} f^l(\mathbf{k}) \nabla_{\mathbf{k}} \cdot \mathbf{u}(\mathbf{k})\, d\mathbf{k} \\ \longrightarrow -\int_{\mathbb{R}^2} f(\mathbf{k}) \nabla_{\mathbf{k}} \cdot \mathbf{u}(\mathbf{k})\, d\mathbf{k} &= \int_{\mathbb{R}^2} \mathbf{u}(\mathbf{k}) \cdot \nabla_{\mathbf{k}} f(\mathbf{k})\, d\mathbf{k},\end{aligned}$$
therefore for the uniqueness of the limit $\nabla_{\mathbf{k}} f^l \rightharpoonup \nabla_{\mathbf{k}} f$ in the weak-$*$ topology.

Now, we prove strong convergence.

Lemma 3. *The limit $f^l \longrightarrow f$ is strong in $L^\infty([0,T], L^1(\mathbb{R}^2))$.*

Proof. Let us consider the difference
$$\varphi^l = f^{l+1} - f^l, \qquad l \in \mathbb{N}. \tag{A.54}$$
This function satisfies
$$\partial_t \varphi^l + \mathbf{u}(t) \cdot \nabla_{\mathbf{k}} \varphi^l + \lambda(f^l)\varphi^l = A(f^l) - A(f^{l-1}) + [\lambda(f^{l-1}) - \lambda(f^l)] f^l. \tag{A.55}$$
Integrating in $\mathbb{R}^2$ we obtain
$$\left\|\varphi^l(t,\mathbf{k})\right\|_{L^1(\mathbb{R}^2)} = \left\|f^{l+1}(t,\mathbf{k}) - f^l(t,\mathbf{k})\right\|_{L^1(\mathbb{R}^2)} \le \int_0^t \left[\left\|U_1(s,\mathbf{k})\right\|_{L^1(\mathbb{R}^2)} + \left\|U_2(s,\mathbf{k})\right\|_{L^1(\mathbb{R}^2)}\right] ds, \tag{A.56}$$
where
$$U_1(t,\mathbf{k}) = A(f^l(t,\mathbf{k})) - A(f^{l-1}(t,\mathbf{k})),$$
$$U_2(t,\mathbf{k}) = [\lambda(f^{l-1}(t,\mathbf{k})) - \lambda(f^l(t,\mathbf{k}))] f^l(t,\mathbf{k}).$$
Further,
$$\begin{aligned}\left\|U_1(t,\mathbf{k})\right\|_{L^1(\mathbb{R}^2)} &\le \int_{\mathbb{R}^2}\int_{\mathbb{R}^2} \left|f^l(t,\mathbf{k}') - f^{l-1}(t,\mathbf{k}')\right| S_\sigma(\mathbf{k}',\mathbf{k})\, d\mathbf{k}'\, d\mathbf{k} \\ &\le C \left\|f^l(t,\mathbf{k}) - f^{l-1}(t,\mathbf{k})\right\|_{L^1(\mathbb{R}^2)}\end{aligned}$$

and, by Proposition 2 (ii),

$$\begin{aligned}\|U_2(t,\mathbf{k})\|_{L^1(\mathbb{R}^2)} &= \left\|[\lambda(f^{l-1}(t,\mathbf{k}))-\lambda(f^l)(t,\mathbf{k})]f^l(t,\mathbf{k})\right\|_{L^1(\mathbb{R}^2)}\\ &\le C_1\left\|\lambda(f^{l-1}(t,\mathbf{k}))-\lambda(f^l(t,\mathbf{k}))\right\|_{L^1(\mathbb{R}^2)}\\ &\le C_1\left\|A(f^{l-1}(t,\mathbf{k}))-A(f^l(t,\mathbf{k}))\right\|_{L^1(\mathbb{R}^2)}+C_1\left\|B(f^{l-1}(t,\mathbf{k}))-B(f^l(t,\mathbf{k}))\right\|_{L^1(\mathbb{R}^2)}\\ &\le 2C_1C\left\|f^{l-1}(t,\mathbf{k})-f^l(t,\mathbf{k})\right\|_{L^1(\mathbb{R}^2)}.\end{aligned}$$

Thus

$$\begin{aligned}\left\|f^{l+1}(t,\mathbf{k})-f^l(t,\mathbf{k})\right\|_{L^1(\mathbb{R}^2)} &\le \tilde{C}\int_0^t\left\|f^l(s,\mathbf{k})-f^{l-1}(s,\mathbf{k})\right\|_{L^1(\mathbb{R}^2)}ds\\ &\le \frac{\tilde{C}^lT^l}{l!}\max_{s\in[0,T]}\left\|f^1(s,\mathbf{k})-f_0(\mathbf{k})\right\|_{L^1(\mathbb{R}^2)},\end{aligned}$$

by recursion, where we have set $\tilde{C} := 2C_1C$. Let $l,m\in\mathbb{N}$ and we consider

$$\begin{aligned}\left\|f^{l+m}-f^l\right\|_{L^1(\mathbb{R}^2)} &\le \left\|f^{l+m}-f^{l+m-1}\right\|_{L^1(\mathbb{R}^2)}+\left\|f^{l+m-1}-f^{l+m-2}\right\|_{L^1(\mathbb{R}^2)}+\cdots+\left\|f^{l+1}-f^l\right\|_{L^1(\mathbb{R}^2)}\\ &\le \sum_{k=0}^{m-1}\frac{(\tilde{C}T)^{l+k}}{(l+k)!}\max_{s\in[0,T]}\left\|f^1(s,\mathbf{k})-f_0(\mathbf{k})\right\|_{L^1(\mathbb{R}^2)}\\ &\le \sum_{k=0}^{\infty}\frac{(\tilde{C}T)^{l+k}}{(l+k)!}\max_{s\in[0,T]}\left\|f^1(s,\mathbf{k})-f_0(\mathbf{k})\right\|_{L^1(\mathbb{R}^2)}\\ &= \sum_{k=l}^{\infty}\frac{(\tilde{C}T)^{k}}{k!}\max_{s\in[0,T]}\left\|f^1(s,\mathbf{k})-f_0(\mathbf{k})\right\|_{L^1(\mathbb{R}^2)}\end{aligned}$$

This implies that

$$\max_{s\in[0,T]}\left\|f^{l+m}(s,\cdot)-f^l(s,\cdot)\right\|_{L^1(\mathbb{R}^2)}\le\max_{s\in[0,T]}\left\|f^1(s,\mathbf{k})-f_0(\mathbf{k})\right\|_{L^1(\mathbb{R}^2)}\sum_{k=l}^{\infty}\frac{(\tilde{C}T)^k}{k!}.$$

The right hand side tends to zero for $l\to\infty$, thus the sequence is a Cauchy one in $L^\infty([0,T],L^1(\mathbb{R}^2))$ therefore the convergence $f^l\to f$ is strong in $L^\infty([0,T],L^1(\mathbb{R}^2))$. □

Now, we can prove Theorem 1.

Since Lemma 3 holds, $f\in L^\infty([0,T],L^1(\mathbb{R}^2))$ is the solution to (3.1). Then, because of Lemma 2, $f\in L^\infty([0,T],W^{1,1}(\mathbb{R}^2))$ and by Lemmas 1 and 2 we have also $(1+|\mathbf{k}|^2)^{\gamma/2}(|f|+|\nabla_{\mathbf{k}}f|)\in L^\infty([0,T],L^\infty(\mathbb{R}^2))$.

It remains to prove the uniqueness for a given control $\mathbf{u}$.

Assume for contradiction that f_1 and f_2 are two solutions of (3.1) with the same initial condition f_0 and all the properties mentioned above. Thus, the function f_1-f_2 satisfies the equation

$$\partial_t(f_1-f_2)+\mathbf{u}(t)\cdot\nabla_{\mathbf{k}}(f_1-f_2)+\lambda(f_1)(f_1-f_2)=A(f_1)-A(f_2)+(\lambda(f_2)-\lambda(f_1))f_2. \tag{A.57}$$

Integration in $\mathbb{R}^2$ and in t gives

$$\begin{aligned}&\|f_1(t,\mathbf{k})-f_2(t,\mathbf{k})\|_{L^1(\mathbb{R}^2)}\\ &\le\int_0^t\left[\|A(f_1(s,\mathbf{k}))-A(f_2(s,\mathbf{k}))\|_{L^1(\mathbb{R}^2)}+\|(\lambda(f_1(s,\mathbf{k}))-\lambda(f_2(s,\mathbf{k})))f_2(s,\mathbf{k})\|_{L^1(\mathbb{R}^2)}\right]ds\\ &\le\int_0^t\left[C\|f_1(s,\mathbf{k})-f_2(s,\mathbf{k})\|_{L^1(\mathbb{R}^2)}+2C_1C\|f_1(s,\mathbf{k})-f_2(s,\mathbf{k})\|_{L^1(\mathbb{R}^2)}\right]ds\\ &=\bar{C}\int_0^t\|f_1(s,\mathbf{k})-f_2(s,\mathbf{k})\|_{L^1(\mathbb{R}^2)}ds,\end{aligned}$$

where $\bar{C}=\bar{C}(S_\sigma)=C(1+2C_1)$. By using Grönwall's inequality, we obtain $\|f_1(t,\mathbf{k})-f_2(t,\mathbf{k})\|_{L^1(\mathbb{R}^2)}=0$. Hence uniqueness.

Appendix B

Proof of Proposition 1.

Proof. Let $(\mathbf{u}_1,f_1)$ and $(\mathbf{u}_2,f_2)$ be two different solutions of problem (3.1). The function f_1-f_2 satisfies the equation

$$\begin{aligned}&\partial_t(f_1-f_2)+\mathbf{u}_1(t)\cdot\nabla_{\mathbf{k}}(f_1-f_2)+\lambda(f_1)(f_1-f_2)\\ &=A(f_1)-A(f_2)-(\mathbf{u}_1(t)-\mathbf{u}_2(t))\cdot\nabla_{\mathbf{k}}f_2+(\lambda(f_2)-\lambda(f_1))f_2.\end{aligned} \tag{B.1}$$

Integration in $\mathbb{R}^2$ and in t gives

$$
\begin{aligned}
&\left\| f_1(t,\mathbf{k}) - f_2(t,\mathbf{k}) \right\|_{L^1(\mathbb{R}^2)} \\
&\leq \int_0^t \left[\left\| A(f_1(s,\mathbf{k})) - A(f_2(s,\mathbf{k})) \right\|_{L^1(\mathbb{R}^2)} + \left\| (\mathbf{u}_1(s) - \mathbf{u}_2(s)) \cdot \nabla_{\mathbf{k}} f_2(s,\mathbf{k}) \right\|_{L^1(\mathbb{R}^2)} \right. \\
&\left. + \left\| (\lambda(f_1(s,\mathbf{k})) - \lambda(f_2(s,\mathbf{k}))) f_2(s,\mathbf{k}) \right\|_{L^1(\mathbb{R}^2)} \right] ds \\
&\leq \int_0^t \left[C \left\| f_1(s,\mathbf{k}) - f_2(s,\mathbf{k}) \right\|_{L^1(\mathbb{R}^2)} + 2CC_1 \left\| f_1(s,\mathbf{k}) - f_2(s,\mathbf{k}) \right\|_{L^1(\mathbb{R}^2)} \right] ds \\
&+ C_T \left\| \mathbf{u}_1 - \mathbf{u}_2 \right\|_\infty \\
&= \bar{C}(S_\sigma) \int_0^t \left\| f_1(s,\mathbf{k}) - f_2(s,\mathbf{k}) \right\|_{L^1(\mathbb{R}^2)} ds + C_T \left\| \mathbf{u}_1 - \mathbf{u}_2 \right\|_\infty ,
\end{aligned}
$$

where $C_T = \int_0^T \left\| \nabla_{\mathbf{k}} f_2(s,\mathbf{k}) \right\|_{L^1(\mathbb{R}^2)} ds$. By using Grönwall's inequality, the claim is proved. □

References

[1] Borzì A, Schulz V. Computational optimization of systems governed by partial differential equations. SIAM Philadelphia; 2012.
[2] Hinze M, Pinnau R, Ulbrich M, Ulbrich S. Optimization with PDE constraints. Mathematical modelling: theory and applications, Springer Netherlands; 2008.
[3] Lions J-L. Optimal control of systems governed by partial differential equations. New York-Berlin: Springer-Verlag; 1971.
[4] Nastasi G, Romano V. Mathematical aspects and simulation of electron–electron scattering in graphene. Z Angew Math Phys 2023;74:28.
[5] Romano V, Majorana A, Coco M. DSMC method consistent with the Pauli exclusion principle and comparison with deterministic solutions for charge transport in graphene. J Comput Phys 2015;302:267–84.
[6] Uehling E, Uhlenbeck G. Transport phenomena in Einstein-bose and Fermi-Dirac gases. I. Phys Rev 1933;43:552–61.
[7] Holstein T. Theory of transport phenomena in an electron-phonon gas. Ann Phys 1964;29:410–535.
[8] Coco M, Majorana A, Romano V. Cross validation of discontinuous Galerkin method and Monte Carlo simulations of charge transport in graphene on substrate. Ricerche Mat 2017;66:201–20.
[9] Majorana A, Nastasi G, Romano V. Simulation of bipolar charge transport in graphene by using a discontinuous Galerkin method. Comm Comp Phys 2019;26(1):114–34.
[10] Nastasi G, Romano V. Discontinuous Galerkin approach for the simulation of charge transport in graphene. Ricerche Mat 2021;70:149–65.
[11] Nastasi G, Camiola V, Romano V. Direct simulation of charge transport in graphene nanoribbons. Commun Comput Phys 2022;31:449–94.
[12] Coco M, Romano V. Simulation of electron–phonon coupling and heating dynamics in suspended monolayer graphene including all the phonon branches. J Heat Transfer 2018;140(9):092404.
[13] Hinze M, Pinnau R. An optimal control approach to semiconductor design, mathematical models and methods in applied sciences. Math Models Methods Appl Sci 2002;12(1):89–107.
[14] Hinze M, Pinnau R. Second-order approach to optimal semiconductor design. J Optim Theory Appl 2007;133:179–99.
[15] Drago C, Romano V. Optimal control for semiconductor diode design based on the mep energy-transport model. J Comput Theor Transp 2017;46(6–7).
[16] Bartsch J, Borzì A, Fanelli F, Roy S. A theoretical investigation of brockett's ensemble optimal control problems. Calc Var Partial Differential Equations 2019;58(5):162.
[17] Bartsch J, Borzì A. MOCOKI: A Monte Carlo approach for optimal control in the force of a linear kinetic model. Comput Phys Comm 2021;266:108030.
[18] Bartsch J, Nastasi G, Borzì A. Optimal control of the keilson-storer master equation in a Monte Carlo framework. J Comput Theor Transp 2021;50(5):454–82.
[19] Breitenbach T, Borzì A. The pontryagin maximum principle for solving Fokker-Planck optimal control problems. Comput Optim Appl 2020;76(2):499–533.
[20] Brockett RW. Notes on the control of the Liouville equation. In: Control of partial differential equations. Lecture notes in math, vol. 2048, Springer, Heidelberg; 2012, p. 101–29.
[21] Jacoboni C. Theory of electron transport in semiconductors. Springer Berlin, Heidelberg; 2010.
[22] Kittel C. Introduction to Solid State Physics, 7th ed. Wiley India Pvt. Limited; 2007.
[23] Castro Neto AH, Guinea F, Peres NMR, Novoselov KS, Geim AK. The electronic properties of graphene. Rev Modern Phys 2009;81:109–62.
[24] Lichtenberger P, Morandi O, Schürrer F. High-field transport and optical phonon scattering in graphene. Phys Rev B 2011;84:045406.
[25] Tomadin A, Brida D, Cerullo G, Ferrari A, Polini M. Nonequilibrium dynamics of photoexcited electrons in graphene: collinear scattering, auger processes, and the impact of screening. Phys Rev B 2013;88:035430.
[26] Borysenko K, Mullen J, Barry E, Paul S, Semenov Y, Zavada J, et al. First-principles analysis of electron–phonon interactions in graphene. Phys Rev B 2010;11:121412, (R).
[27] Li X, Barry E, Zavada J, Buongiorno Nardelli M, Kim K. Surface polar phonon dominated electron transport in graphene. Appl Phys Lett 2010;97:232105.
[28] Landauer G, Jimenez D, Gonzalez J. An accurate and verilog-a compatible compact model for graphene field-effect transistors. IEEE Trans Nanotechnol 2014;13(5):895—904.
[29] Mustieles F. Global existence of solutions for the nonlinear Boltzmann equation of semiconductor physics. Rev Mat Iberoam 1990;6:43–59.
[30] Gel'fand I, Shilov G. Generalized Functions, vol. 1–5, Academic Press; 1966-1968.
[31] Brockett R. Control of partial differential equations. vol. 2048, Heidelberg: Springer; 2012, p. 101–29.
[32] Cheng Y, Gamba IM, Majorana A, Shu C-W. A brief survey of the discontinuous Galerkin method for the Boltzmann-Poisson equations. SeMA J 2011;54(1):47–64.
[33] Hager W, Zhang H. A survey of nonlinear conjugate gradient methods. Pac J Optim 2006;2:35–58.
[34] Degond P. Global existence of smooth solutions for the Vlasov-Fokker-Planck equation in 1 and 2 space dimensions. Ann Scient EC Norm Sup 1986;19:519–42.
[35] Evans LC. Partial differential equations. Providence, R.I.: American Mathematical Society; 2010.